International Journal of Earth Sciences (2022) 111:675–701
https://doi.org/10.1007/s00531-021-02141-6

ORIGINAL PAPER

Ordovician submarine to subaerial volcanism along the western Gondwana margin: records of the Famatinian belt evolution, north-western Sierras Pampeanas, Argentina

Clara Eugenia Cisterna[1,2] · **Beatriz Coira**[1,3]

Received: 9 December 2020 / Accepted: 18 November 2021 / Published online: 25 January 2022

Abstract
The Suri-Las Planchadas Volcanic-Sedimentary Complex (SPVSC), northwest of the Sierras Pampeanas in Argentina, comprises an Early to Middle Ordovician (Floian–Dapingian) submarine and subaerial succession with a variety of mafic to felsic volcanic lithofacies. These units include mafic to intermediate submarine massive-hyaloclastic lava flows, dacitic lavas, pyroclast-rich volcaniclastic deposits, intrusions of domes/sills and rhyodacitic—rhyolitic lavas. Along Las Planchadas hill a section of ~ 3 km thickness is exposed showing vertical and lateral variations. The lower part is dominated by massive, pillowed and basaltic to intermediate lavas, autobreccia and hyaloclastic facies, representing the beginning of the volcanic arc activity. The upper almost 2 km of the succession is dominated by subaqueous-resedimented volcaniclastic siltstones, sandstones and breccias with abundant pyroclastic components and rhyodacitic to rhyolitic lava-domes, sills and dykes. Tuff and ignimbrite lithoclasts, abundant shards and pumice fragments were determined in the resedimented deposits. Volcanism in the SPVSC started with submarine eruptions and progressively grew above the wave base, accompanied by a change from mafic to intermediate and felsic members. The eruptive pattern shifted from effusive to explosive, producing a large apron of syn-and post-eruptive volcaniclastic deposits of debris flows and turbidity currents. They are the evidence of variations in composition and volcanic styles and their development contributed to generate an apron surrounding the volcanoes. The apron prograded and aggraded with the evolution of the volcanism culminating in shallow water volcanogenic beds. The final phase was characterized by felsic subaerial or shallow subaqueous explosive volcanism.

Keywords Ordovician volcanism · Submarine emplacements · Mass-flow deposits · Arc-back arc

Introduction

The study of volcanic deposits along active margins provides an excellent tool to understand geodynamic processes linked to tectonic evolution. Such processes can be understood from compositional, lithofacial and textural studies of the volcanic deposits (Allen et al. 2007). The Suri-Las Planchadas Volcanic-Sedimentary Complex (SPVSC), that build up the Las Planchadas and Narváez hills (Fig. 1b), and form part of the proto-Andean margin, represents a well exposed example of the top of the Famatinian arc with a complete record of the volcanic activity during the Early to Middle Ordovician. Lithofacies analysis based on features as composition, textures and structures of these ancient successions give insights on the emplacement mechanisms and eruption styles of volcanism under subaqueous-subaerial environment during the evolution of the Famatinian arc, applicable throughout its extension for more than 6000 km from Venezuela to northeast Patagonia as was indicated by Pankhurst et al. (2006), Chew et al. (2007), Van der Lelij et al. (2016), García-Ramírez et al. (2017), among others. Likewise, this work attempts to contribute elements of analysis for the understanding of other ancient volcanic successions that,

✉ Clara Eugenia Cisterna
claracisterna@csnat.unt.edu.ar

Beatriz Coira
bcoira2015@gmail.com

1 Consejo Nacional de Investigaciones Científicas y Técnicas, Buenos Aires, Argentina

2 Facultad de Ciencias Naturales, Universidad Nacional de Tucumán, Miguel Lillo 205, 4000 Tucumán, Argentina

3 Instituto de Ecorregiones Andinas (INECOA), CONICET-Universidad Nacional de Jujuy, Instituto de Geología y Minería, Av. Bolivia 1661, 4600 San Salvador de Jujuy, Argentina

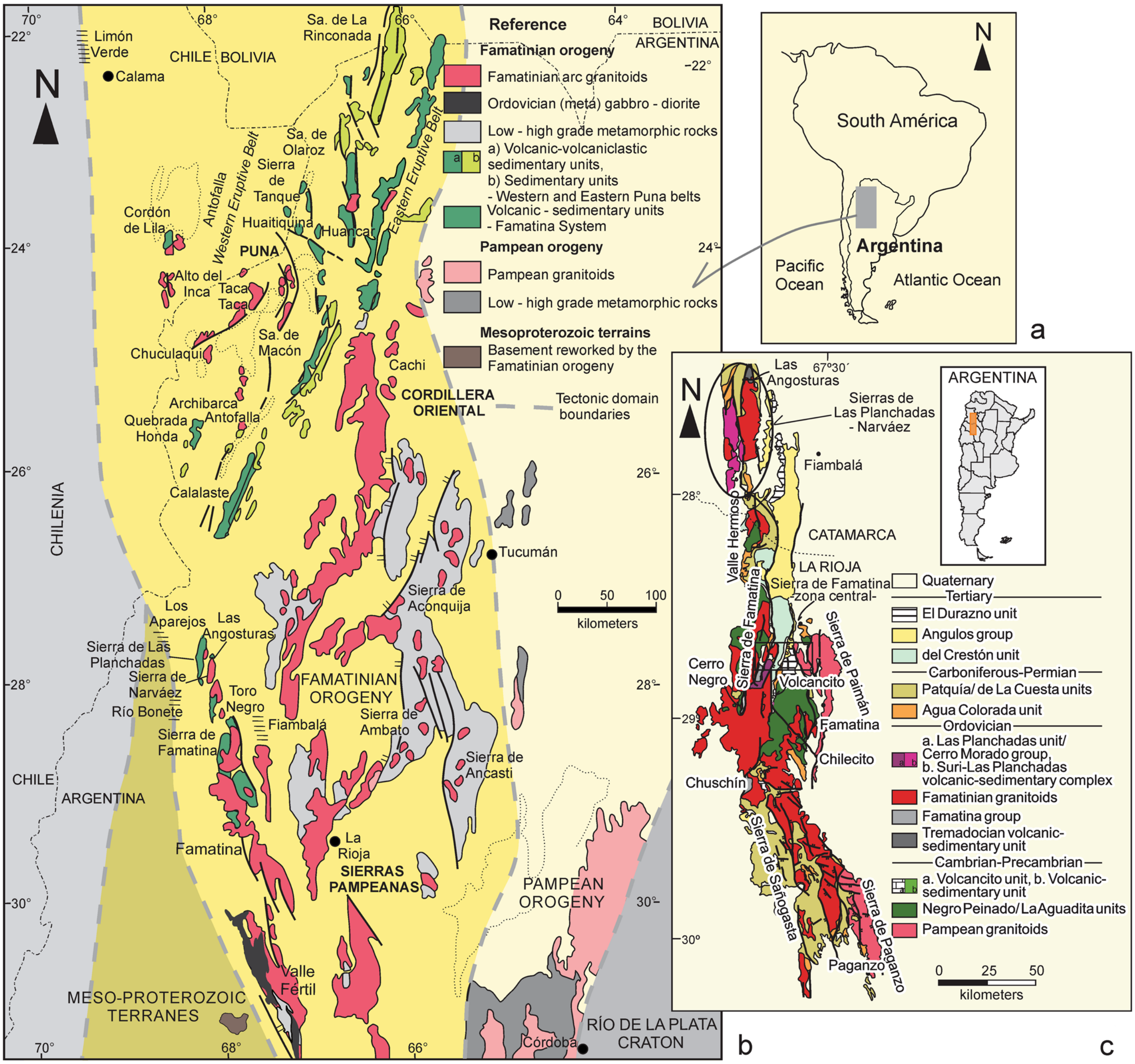

Fig. 1 **a** Simplified map of South American showing the position of Fig. 1b. **b** Famatinian orogen in Sierras Pampeanas. The boundaries of the regions are modified from Ramos (2018) and the Puna Ordovician outcrops are from Coira et al. (2009). **c** Geologic map of the Famatina System (modified from Cisterna and Coira 2017)

like the SPVSC, represent relics of volcanic centers that evolved under subaqueous and subaerial conditions in similar tectonic settings.

The Famatinian Orogeny, ranging from the early to middle Ordovician as was defined by Aceñolaza and Toselli (1976), includes widespread regional metamorphism and arc magmatism related to an active continental margin. Extending from north to south for more than 400 km between 27° and 36° S in the northwest of Argentina, the Famatinian belt (Astini and Dávila 2004) represents a continuous and fast overlapping of high-to medium-and low-grade metamorphism episodes, deformation, anatexis, magmatism and mineralization during the Early Paleozoic times. The western units along the belt, are characterized by Late Cambrian to Early-Middle Ordovician volcanism intercalated with marine and volcaniclastic successions and Early to Middle Ordovician I-and S-type intrusions (Fig. 1a, b). From this context, Las Planchadas and Narváez hills form the northern portion of the Famatina System "sensu" Petersen and Leanza (1953) and are considered upper levels of the Famatinian arc (e.g., Rapela et al. 2018).

Previous descriptions and interpretations of the SPVSC published by the authors, have focused on stratigraphic aspects and local petrographic and geochemical studies as tools to explain specific source processes. The volcaniclastic facies, studied by Cisterna and Coira (2014) east to west along the Chaschuil section, are reorganized and redefined at the present work according new data from other analysed localities as the outcrops at the southern portion of the Las Planchadas hill or to the north, in the Agua del Médano area. Volcanic facies features and origin, internal architecture and related volcanic processes in the context of the Famatinian arc tectonic evolution are still a topic for discussion. This work analyses the volcanic facies characteristics and distribution, focusing on styles of volcanic activity and sedimentation. Detailed facies analysis is based on mapping and profiles across the Las Planchadas and Narváez hills, and takes into account new data, previous works and the regional structures affecting the area.

Geologic setting and stratigraphic framework

The Famatinian orogeny, restricted from the Late Cambrian to the Middle Ordovician (Astini and Benedetto 1993; Astini et al. 1995; Pankhurst et al. 1998), records the subduction of oceanic lithosphere along the western margin of Gondwana and its tectonic evolution is supported by paleontological, petrological, geochronological and paleomagnetic data (Aceñolaza and Toselli 1976; Lork and Bahlburg 1993; Kraemer et al. 1995; Dalziel 1997; Astini and Dávila 2004; Bierlein et al. 2006; Viramonte et al. 2007; Chernicoff et al. 2010; Ramos 2018, among others).

The Famatinian arc-back arc in northwest Argentina (490–430 Ma; Rapela et al. 1998) appears in a series of discontinuous north to south mountain blocks, over 1000 km (between 22°S and 33°S; Coira et al. 2009). In Puna and the north segment of the Famatina System, it is represented by intrusive and volcanic rocks related to volcaniclastic turbidity and debris flow deposits (e.g. Bahlburg 1990, 1998; Coira and Pérez 2002; Pankhurst et al. 1998; Bierlein et al. 2006; Cisterna and Coira 2014; Bahlburg et al. 2016). Volcanism and sedimentation age ranges from late Cambrian to Early–Middle Ordovician (485–444 Ma; Bahlburg 1990, 1991; Viramonte et al. 2007; Cisterna and Coira 2014; Cisterna et al. 2017). To the east of the Famatinian arc, the back-arc region is characterized by the development of HT metamorphism (peak conditions of c. 4–6 kbar and 670–820 °C), mainly developed between c. 505–460 Ma (Larrovere et al. 2019). It is almost coeval with the peak emplacement of the magmatic arc activity at c. 485–465 Ma (Ducea et al. 2010; Rapela et al.2018; Larrovere et al. 2019).

For the Famatina Range (running at the central sector of the NW Argentina Famatinian Belt), a volcanic arc was initially suggested by Aceñolaza and Tosselli (1984). Subsequently, some authors have favored a back-arc model for that belt on a petrological basis (Mannheim 1993; Clemens 1993 and Toselli et al. 1996). Isotopic and geochemical studies on the Famatina Early Ordovician granitoids document the evolution of a magmatic arc on thickened continental crust (Pankhurst et al. 2000), instead of a genesis under an island arc regime with subduction of oceanic crust under oceanic crust. A northward extension of this magmatic arc, along the Puna magmatic belt has been postulated by Coira (1979), Coira et al. (1982), Ramos (1988), Loewy et al. (2004), Chew et al. (2007), Bahlburg et al. (2011) and Cisterna et al. (2017), among others. A continental magmatic arc (the Famatinian magmatic arc) between 21° and 26° S with a north-easterly directed subduction zone and developed on continental crust was proposed by Niemeyer et al. (2017) for the Ordovician volcanic records of north Chile-Argentina Andes. Taking into account the geochemical study of the basic volcanism developed along the Las Planchadas and Narváez hills, a transition from an island arc to a back-arc along an overriding plate progressively thicker was postulated by Cisterna et al. (2017).

Las Planchadas and Narváez hills are mainly composed of Paleozoic units, with ages established according to their geological relations, fossil content and geochronological data (Fig. 1c). The older rocks are Tremadocian volcanic-sedimentary deposits due the presence of graptolites pointing this age (Cisterna and Coira 2017) and they are intruded by the Las Angosturas Granodiorite of 485 ± 7 Ma in age (Rubiolo et al. 2002). The most extended deposits are represented by the Suri-Las Planchadas Volcanic-Sedimentary Complex (SPVSC) (Cisterna and Coira 2017) (Figs. 2, and 3), having a brachiopod-rich fauna associated with trilobites and conodonts in the Chaschuil area. They allow to assign these units to the Floian–Dapingian (Albanessi and Vaccari 1994; Benedetto 1994; Vaccari and Waisfeld 1994).

The Tremadocian volcanic-sedimentary unit shows low-grade metamorphism mineral associations, a main S_1 discontinuous cleavage and locally complex structures (F_1 and F_2 folds) denoting penetrative polyphasic deformation. This contrasts with the simple structure (mainly open folds) of the Floian-Dapingian succession and without evidence of metamorphism (Cisterna and Mon 2014). Taking into account that subduction zones are characterized by margin-parallel active arc volcanoes together with wide hot back-arcs as one of its fundamental characteristic (Currie and Hyndman 2005), Altenberger et al. (2021) propose that the Ordovician volcano-sedimentary sequences outcropping at the Sierras de Narváez and Las Planchadas may represent the volcanic

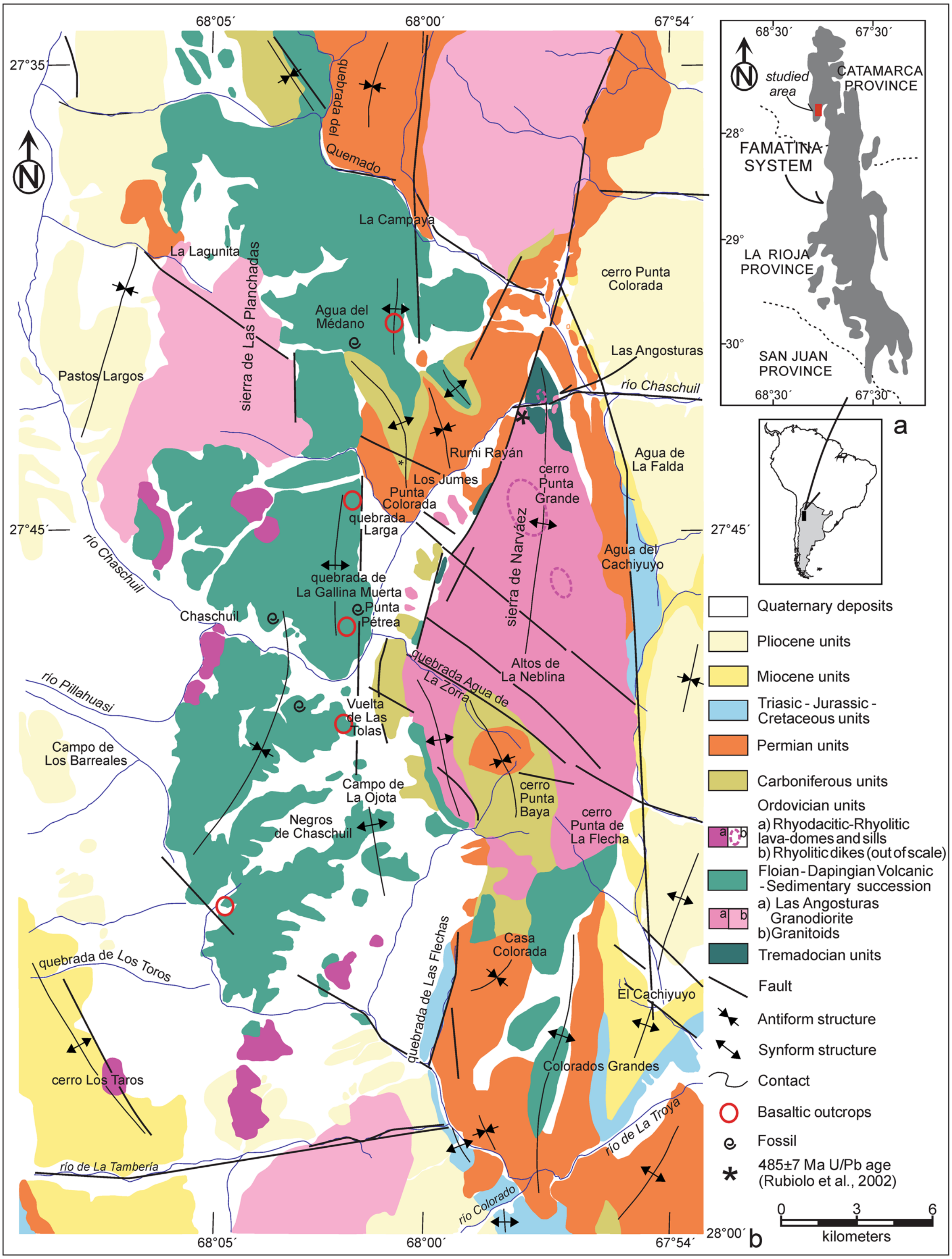

Fig. 2 **a** Geological tectonic setting of the Las Planchadas–Narváez hills, NW Argentina. **b** Las Planchadas and Narváez hills geological map (modified from Cisterna and Coira 2017)

arc while the Sierras de Aconquija, Ancasti, Ambato running parallel ca. 200 km to the east (composed of HT metamorphic rocks yielding the same ages) (Fig. 1b) take part of the hot back-arc region. The Ordovician volcanic successions are covered, above an unconformity, by thick siliciclastic continental units of the Late Paleozoic (Fig. 3).

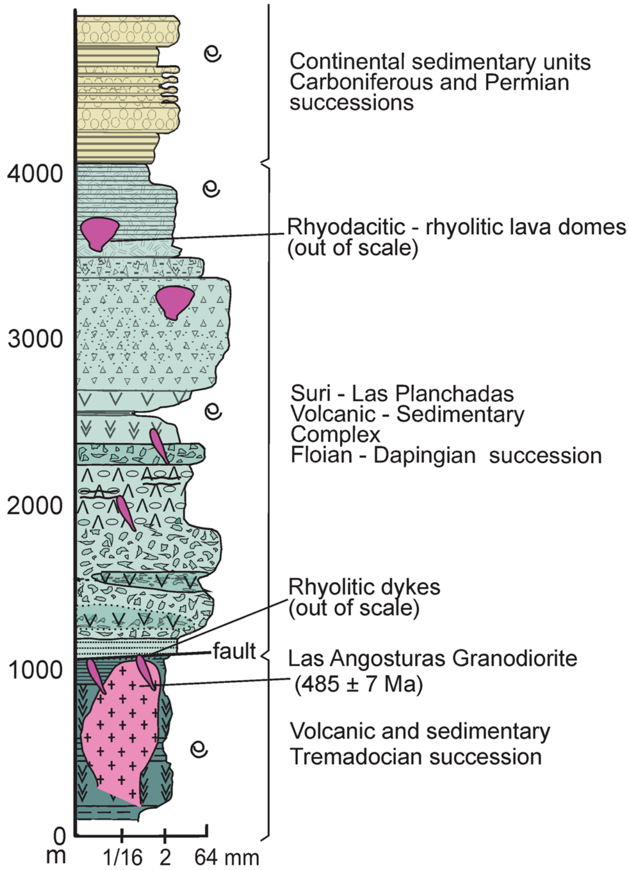

Fig. 3 Generalized stratigraphic column of the Las Planchadas–Narváez hills

Suri-Las Planchadas volcanic-sedimentary complex

Internal stratigraphy

On the basis of previous mapping and stratigraphic studies of the area (Cisterna and Coira 2014, 2017; Cisterna et al. 2017) together with new data, the present contribution defines field relations, distribution, compositional and textural variations that characterize the volcanic and volcaniclastic Ordovician deposits of the Suri-Las Planchadas Volcanic-Sedimentary Complex (SPVSC). This knowledge is useful to define/or redefine the main lithofacies, establishing their spatial and temporal distribution and significance. In order to analyze these characteristics in the Complex, affected by folds and later faulting, sections have been documented which display relatively continuous outcrops and free of structural repetition. Detailed information of the main sections, from north to south, are presented in Table 1 and Figs. 4 and 5.

Taking into account the different analysed sections and other representative outcrops along the Planchadas and Narváez hills, the Ordovician succession can be divided into a lower portion (1000 m thick) of mafic to intermediate lava dominant with minor fragmental facies; and an upper one (2000 m thick) dominated by volcaniclastic units with minor felsic lavas (Fig. 3). The first portion, composed of basaltic to basaltic andesite lavas (locally pillowed) and related hyaloclastites and pillow breccias, mainly outcrops along a nearly north to south oriented area (Fig. 2). The upper portion is dominated by volcaniclastic deposits, principally formed by breccias, interspersed with finer volcaniclastic sedimentary levels (psammitic and pelitic) with lavic, pyroclastic and rarely non-volcanic clasts. Rhyodacitic and rhyolitic lava domes are emplaced among them and the lithostratigraphic succession is intruded by small-volume rhyolitic sills and dikes, especially at the south—southwestern of the area (Fig. 2). Doleritic dykes/sills are also interbedded among the succession (e.g. Chaschuil section), indicating that basic volcanism continued throughout the development of the volcanic complex. About the fossil records, the main outcrops were studied in two localities along the Chaschuil area (Fig. 2), where were defined the brachiopods associated with trilobites and conodonts (Albanessi and Vaccari 1994; Benedetto 1994; Vaccari and Waisfeld 1994; Mangano and Buatois 1996) hosted in yellow siltstones to fine sandstones beds of the volcaniclastic sedimentary levels. At the Punta Pétrea area were found Ordovician brachiopods (Paralenorthis riojanus, Famanorthis turneri and Tritoechia sp.) in volcaniclastic sandstones interbedded with lapilli rich fine to medium sandstones (Cisterna et al. 2010) and to the north, in the southwest of the Agua del Médano, outcrops fine sandstones hosting brachiopods and trilobites (Fig. 2).

Terminology

Facies terminology used here is taking into account McPhie et al. (1993), McPhie (1995) and Allen et al. (2007). Volcanic deposits are classified into coherent and volcaniclastic, according to their original textures. Coherent volcanic facies resulting from cooling and solidification of magma in aerial, subaerial and subaqueous conditions may be associated with autoclastic and hyaloclastic breccias (McPhie et al. 1993). The volcaniclastic term is descriptive and applies to deposits mainly composed of volcanic particles (Fisher 1961), including four main genetic categories: autoclastic, pyroclastic, resedimented and volcanogenic sedimentary rocks (McPhie et al. 1993).

Lithotypes

The Suri–Las Planchadas Volcanic-sedimentary Complex (SPVSC) displays a great variety of lithotypes, whose characteristics are summarized in Tables 2, 3, 4 and 5.

Table 1 General characteristics of the main analysed sections

Section	Description
Agua del Médano section (27° 40′ 50″ S–67° 58′ 51″ W and 27° 40′ 21″ S–68° 00′ 30″ W)	NW–SE sequence dipping to the east and conforming the eastern flank of a 3 kms axial long anticline (Fig. 2). It represents approximately 150 m of the Arenigian column mainly composed by volcaniclastic deposits and basalts. The base of the section is not see in the area and the upper portion is covered by Upper Paleozoic units and recent sands deposits (Fig. 4c)
North Quebrada Larga section (27° 44′ 01″ S–68° 01′ 43″ W and 27° 45′ 15″ S–68° 01′ 42″ W)	It builds up an anticline structure, whose axis is sub-horizontal, with north–south trend for 5 km (Fig. 2). The base of the section is poorly exposed to the east, where locally an irregular contact can be observed between the basalt and a yellow siltstone. The section is mainly composed by basalts and their hyaloclastic equivalents and it was detailed studied by Cisterna et al. (2017) (Fig. 4a)
South Quebrada Larga–Punta Pétrea section (27° 46′ 07″ S–68° 01′ 09″ W and 27° 46′ 23″ S–68° 02′ 47″ W)	It extends from north to south forming the eastern flank of an anticline (Fig. 2). It builds nearly 1300 m of the Ordovician column and is composed by basaltic, andesitic and dacitic lavas, hyaloclastic facies and volcaniclastic resediment breccias, together with psamitic and pelitic volcaniclastic sedimentary members containing pyroclastic material levels (e.g. abundant accretionary lapillis). The fossil content testifies the Floian–Dapingian age of the sequence (Fig. 4b)
Chaschuil section (27° 47′ 23″S–68° 04′ 37″W and 27° 48′ 58″S–68° 01′ 45″W)	It develops an east to west continuous succession of outcrops along nearly 5 kms in the Chaschuil area (Fig. 2). This section builds up a synclinal structure, whose axis is sub-horizontal, with a north to south trend. The base of the profile is poorly exposed in the western outcrops, where locally can be seen an irregular contact between a dacitic lava and a green mudstone. The top of the profile, at the east, has facies laterally equivalent to the Vuelta de Las Tolas member described by Mángano and Buatois (1997) at the homonymous locality. At the southeast Chaschuil area, the beds of the Vuelta de Las Tolas member are overlaying basaltic lavas forming the core of the Vuelta de Las Tolas anticline (Cisterna and Coira 2014; Cisterna et al. 2017) (Fig. 5). The succession studied is characterized in its basal level by a dacitic lava member, succeeded by abundant volcaniclastic breccias, sandstones, mudstones and siltstones bearing abundant pyroclastic components. These members are immediately followed by volcaniclastic sedimentary lithofacies. Towards the top the pelitic levels have a Floian–Dapingian brachiopod fauna (Benedetto 1994)

Basaltic lavas (*BaL*)

Lobate basaltic flows more than 10 m thick, develop rapid lateral and vertical variations, turning from massive into autoclastic, composed by highly fractured basalts and developing jigsaw-fit textures (Fig. 6a–c). The blocky fragments are larger than 10 cm, most of them have curviplanar fracture surfaces; no chilled margins are observed. Excellent outcrops occur along the north Quebrada Larga section (Figs. 2, and 4a), where basalts are emplaced in massive to laminate yellow siltstones and fine sandstones. The contact related to the Monomictic Basaltic breccias (*BaBr/m*) is often transitional.

Pillowed basalts develop relatively small outcrops and are locally related with pillow-breccias. Siltstones and sandstones, comprising centimetre to decimetre beds, planar to wedge-shaped form, are common overlying the top of the lavas and breccias. The Agua del Médano section (Figs. 2 and 4c) is a good example of these rocks (Fig. 7b).

Interpretation: the preserved structural and textural characteristics in basaltic lavas related to the intensively fractured portions, with the development of autoclastic facies with jigsaw-structures and other characteristics above described (blocky clasts with curviplanar fracture surfaces and non-quenched margins) may be awarded to non-explosive magma-water interaction processes (cf. Carr and Jones 2001). Basaltic flows that are cooler and more viscous and/or subjected to locally higher strain rates than other emplacements of massive basalts, commonly react to stress in a brittle mode. They develop blocks of lava, located at the margins of the lava bodies or dislodged by continuous movement of the flow (cf. McPhie et al. 1993). Basaltic pillow lavas associated with pillow breccias are also pointing to non-explosive magma-water interaction.

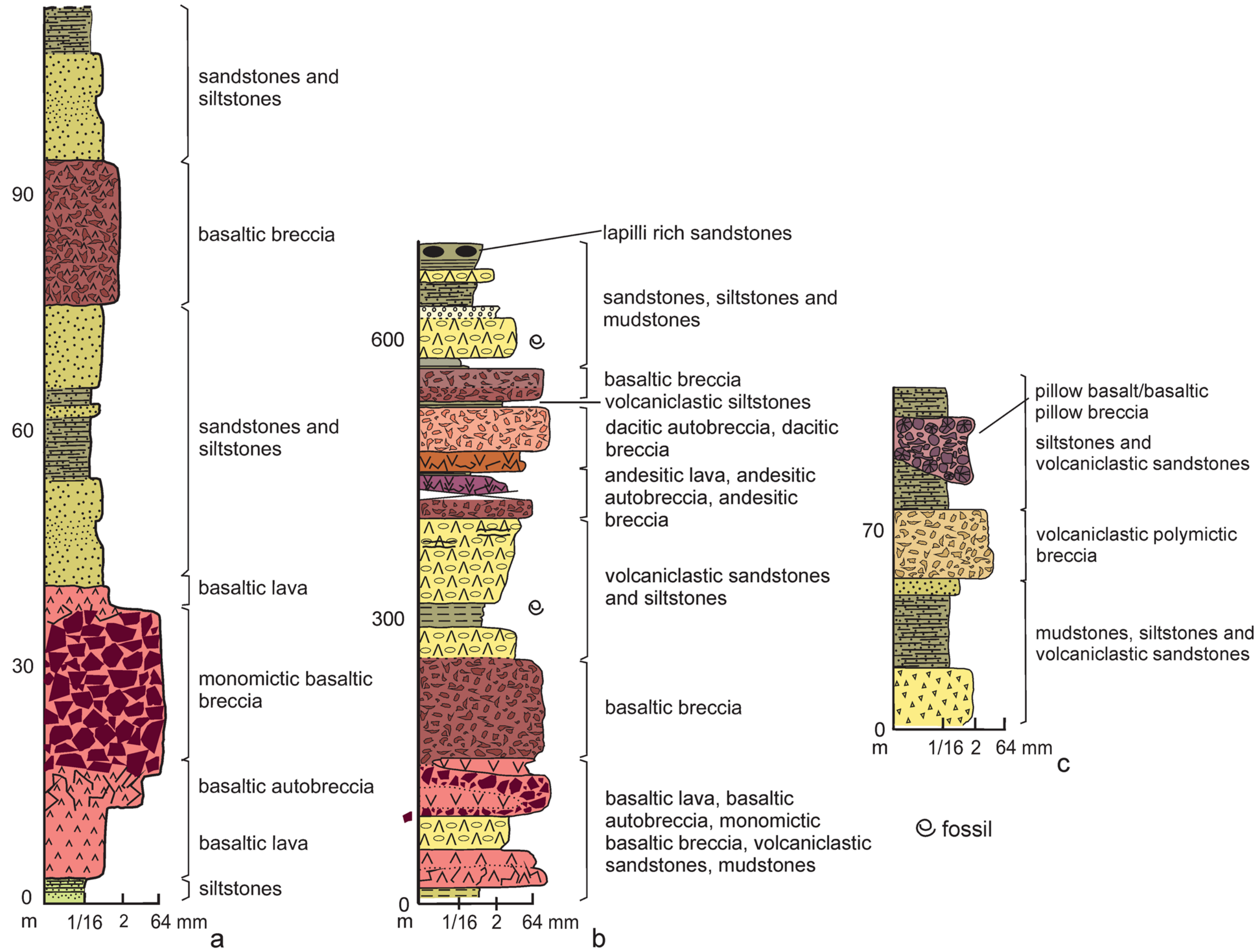

Fig. 4 Simplified logs of the **a** North Quebrada Larga section (modified from Cisterna et al. 2017); **b** South Quebrada Larga–Punta Pétrea section (modified from Cisterna and Coira 2017); **c** Agua del Médano section

Monomictic basaltic breccias (*BaBr/m*)

They develop deposits up to 60 m thick and are in transitional or sharp contact related to the autoclastic basalts (Fig. 6a, d). Its remarkable features are the randomly oriented clasts showing flow foliated slabs with jagged ends, ragged and blocky clasts with curviplanar surfaces and quenched margins; scarce matrix and development of jigsaw texture.

Interpretation: Monomictic basaltic breccias, characterized by a wide range in size of the clasts and their particularly shapes (see above and in Table 2) together with the presence of clasts with quenched margins and jigsaw structure, may result from the quench fragmentation during the disintegration process of lava-flow subaqueous emplacements. Quenching achieves fractures affecting the lavas and clasts are formed in situ by the fracturing and spalling of quenched glass fragments (cf. McPhie et al. 1993). In accordance with this, monomictic basaltic breccias are in situ hyaloclastites. Jigsaw textures are pointing to that clasts remain in place while being fragmented (cf. McPhie et al. 1993).

Basaltic pillow breccias (*BaPilBr*)

They form lensoidal deposits, no more than 8 m thick and 20 m long, interbedded with fine sandstones and mudstones (eg. Agua del Médano section) (Fig. 8a). They are almost always together with pillow lava emplacements and are characterized by the presence of rounded or sub-rounded pillow clasts up to 1 m, that may preserve chilled margins. Breccia shows a great variety of clasts sizes and is unstratified. Locally, the hosting sedimentary rocks could be recognized, partially incorporated into the breccias or forming enclaves in the basaltic pillows. This sedimentary material is commonly altered (silicified) (Fig. 6e).

Interpretation: the interaction with the sedimentary host, generating its fragmentation with the inclusion of altered

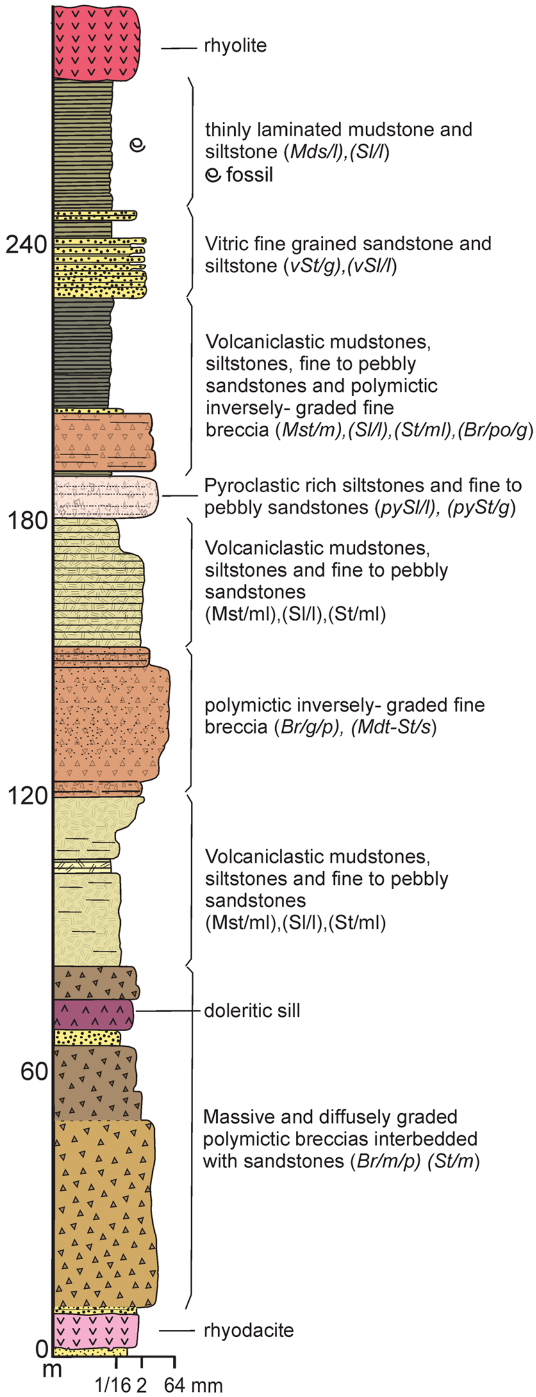

Fig. 5 Simplified logs of the Chaschuil section (modified from Coira and Cisterna 2014)

fragments in the breccia and enclaves in the lavas, together with the development of stratified layers at the upper portions of these rocks indicate the intrusive character of the lavas. Emplacements of lavas that disturb or destroy the pre-existing stratification, incorporating and altering or hardening fragments of the host sedimentary rocks, together with presence of sedimentary beds developed at the tops of them (without any alteration) is indicative of pillow lava intrusions (cf. McPhie et al. 1993). Pillow breccias may be locally developed very near to the dismembered lava.

Basaltic breccias (*BaBr*)

Occurring as beds and lenticular beds up to 20 m thick, laterally discontinuous (100 m long), are interbedded with sandstones (medium to fine grained) and siltstones (Fig. 9). The breccias have sharp basal contacts, are massive and rarely have a diffuse stratification. They are clast-supported with angular to subangular basaltic clasts up to 60 cm (Fig. 8b, c). Locally, elongate clasts show a weak long-axis clast imbrication. The matrix is commonly a poorly-sorted fine psammite.

Interpretation: basaltic breccia (*BaBr*), characterized by unsorted and commonly poorly or unstratified deposits, suggest rapid resedimentation along steep slopes. Locally, clast imbrication and/or basal scours (granule sandstone within breccia) may be indicating flow turbulence (cf. Lowe 1982).

Andesitic and dacitic lavas (AnDaL) and Andesitic and dacitic breccias (AnDaBr)

Andesitic and lesser amounts of dacitic lavas are massive and form lenticular bodies up to 20 m thick, locally fragmented developing breccias. Outcrops are scarce and were recognized at the south of the Quebrada Larga section (Figs. 4b, and 6f).

Interpretation: andesites and dacites form coherent lava, partly in situ brecciated, transitionally varying to the breccias of the same composition. Breccias have clasts up to 70 cm, angular to subangular, arranged with a jig-saw texture and with no evidence of rotation. The characteristics of the breccias, as were described for the basaltic ones, point to a subaqueous emplacement developing in situ hyaloclastites.

Rhyodacitic and rhyolitic lava-domes/sills (Rhyod-Rhyol/Ld-s) and Rhyolitic dykes (Rhyol/d)

Rhyodacitic and rhyolitic lava-domes/sills (*Rhyod-Rhyol/Ld-s*). Lenticular bodies (nearly 10 m thick and up to 30 m long) are intercalated within volcaniclastic facies. Although contact heat reactions could not be defined, the low ratio long–width, the shape and sharp top contacts of these units allow to define them as sills (Fig. 10a). Rhyodacites and rhyolites are also defining small domes (50 m diameter) (Fig. 10b). They are commonly red to pink, porphyritic, characterized by a variably crystal-rich ratio, massive and flow-banded structure (Fig. 10c, d) that commonly show portions with a red oxidized ground mass (Fig. 10e). The contact of the domes is sharp and locally displayed small brecciated portions at the top (Fig. 10f).

Table 2 Basic to intermediate lavas and their fragmented equivalents facies: summary

Lithotype	Code	Description
Basaltic lavas	(*BaL*)	Greenish black rocks, commonly massive and locally developing flow foliation structure. Fine-grained and porphyritic, the matrix shows crystallinity variations. Vesicles (2 mm–2.5 cm) are irregular and generally oriented according the main foliation. Phenocrysts (5–12%) are plagioclase (up to 3 mm) (30%) and clinopyroxene, commonly augite and augite-diopside (up to 1 mm) (1.5%). Microphenocrysts of olivine, partially replaced by pyroxene and/or amphibole, are also common. The matrix displays pilotaxitic texture and less common ophitic or subophitic. Glass groundmass may be fresh or partially altered into palagonite and have plagioclase microlites weakly to moderately aligned and defining around phenocrysts morphologies as swallow-tail terminations. Augite, olivine and opaque minerals are also common in the matrix. Vesicles may be filled with calcite, quartz and/or chlorite Basaltic pillow lavas form lenticular bodies of nearly 8 m thick and occasionally, pillows display multiple rind structures (Fig. 7c, d). They developed interaction textures with the hosting and locally appear C-shape pillow lobes with segments showing black glassy chilled rinds, locally flowing wrinkled (Fig. 7e, f)
Monomictic Basaltic breccias	(*BaBr/m*)	Poorly sorted breccias with randomly oriented clasts, which shapes vary between flow foliated slabs with jagged ends, ragged or blocky clasts with curviplanar surfaces (Fig. 6a, d), commonly displaying jigsaw texture. The clasts occasionally develop quenched margins and glassy rims. Their size varies in different sectors (from less than one mm up to 50 cm), usually larger near the massive lavas. The groundmass is scarce, composed of glassy particles and phenocryst fragments (plagioclase), carbonate and palagonite. Clasts may be of highly vesiculated basalts (Fig. 6a)
Basaltic breccias	(*BaBr*)	Breccias are composed by angular to subangular basaltic clasts, having different size and reaching 60 cm in diameter (Fig. 8b, c). The poorly-sorted matrix, commonly of a fine sandstone (mainly composed by fragments of basalts and plagioclase crystalloclast) show lesser content of mudstone. Basaltic clasts display different structures, the most frequent have a vitric groundmass, sometimes altered to palagonite, with thin plagioclase laths in a pilotaxitic groundmass and elongated or subrounded vesicles, aligned parallel to the long axis of the clasts, and filled by carbonate or chlorite. Other basaltic clasts may be rounded and subrounded, with quenched margins and a groundmass composed by glass or oxidized glass, feldspar microlites and vesicles filled by carbonate, chlorite and quartz; phenocrysts, sometimes fractured, are plagioclase and augite
Basaltic pillow breccias	(*BaPilBr*)	Clast-supported breccias in sharp contact with a fine psammitic and mudstone unit. Breccias are unstratified and unsorted, with basaltic clasts rounded to sub-rounded that display a range of size between few centimeters to 1 m, locally preserving quenched margins. Matrix is scarce and the sediments hosting may be included in the breccia and altered
Andesitic and dacitic lavas	(*AnDaL*)	Andesites (or basaltic andesites) are dark grey to greenish, porphyritic texture with plagioclase phenocrysts (less than 2 mm large) and microphenocrysts of augite and hornblende in a glassy or very fine fluidal groundmass. Hornblende and the glassy-groundmass are altered by chlorite and calcite Dacites are greenish–green, display porphyritic texture with hornblende and plagioclase phenocrysts (20%) ranging from 4 to 2 mm large. Scarce (<5%) and smaller quartz phenocrysts (1 mm) and biotite. Groundmass composed by fine aggregates of quartz and plagioclase developing microfelsitic texture, with irregular vesicles (5%). Ferromagnesian minerals are commonly replaced by chlorite
Andesitic and dacitic breccias	(*AnDaBr*)	The fragmented andesites and dacites show clasts of millimeters to 70 cm, angular to subangular forming coarse to fine clast-supported breccia and arranged with a jig-saw texture and with no evidences of rotation. Fragments are immersed in a scarce fine matrix commonly chloritized

These rocks usually have abundant small (mm) to medium (up to 1.5 cm) spherulites generating apparent granular texture. Recrystallization of originally glassy sectors in rhyolites, usually along flow foliation directions, gave these rocks fine banded structure (Fig. 10f). Chlorite alteration of the matrix turns rhyolites into grey colours.

Rhyolitic dykes (*Rhyol/d*). Bodies are discontinuous, tabular or developing lenses with up to 50 m long, in a sharp contact related to the host. These rocks are characterized by their granophyric and spherulitic textures, better to see at microscopic scale. For petrographic characteristics of rhyodacitic and rhyolitic members see Table 3.

Interpretation: textural characteristics (e.g. porphyritic texture, euhedral phenocrysts and the unbroken and euhedral phenocrysts, microcrystalline groundmass) together with the bodies morphology, sharp contact and flow banding structure point to define the rhyodacitic and rhyolitic lava bodies as domes. Sills are scarce and recognized as lenticular emplacements within the volcaniclastic units. The rhyolitic dykes are discordant in the Ordovician succession.

Table 3 Rhyodacitic and rhyolitic lava domes/sills and rhyolitic dykes: summary

Lithotype	Code	Description
Rhyodacitic–rhyolitic lava-domes and sills	(*Rhyod-Rhyol/Ld-s*)	Red to dark red, porphiritic texture, feldspars and quartz phenocrysts (20–30%) (0.5–1 cm). Plagioclase developed glomeroporphyritic aggregates and quartz are resorbed with deep embayments. Scarce biotitic micro-phenocrysts (˂ 1%). Fine-grained quartz-feldespatic micropoikilitic matrix, locally show flow-banding texture. Groundmass, dominated by anhedral quartz and feldspars, with spherulites interspersed. The last ones are composed of fine radiating needles of quartz and feldspar and reach up to 2 cm. Some spherulites form clusters of two or three. Between spherulites are fine sheets of chlorite, white mica and biotite, together with quartz, epidote and opaques. Chlorite, calcite and/or quartz are filling vesicles (up to 1 mm)
Rhyolitic dikes	(*Rhyol/d*)	Dykes are characterized by a nearly homogeneous groundmass with granophyric texture and spherulites. The granophyric intergrowth show blebs, patches and threads of quartz in a feldspar base. Spherulites are composed of relatively long feldspar laths and are surrounded by granophyric intergrowth

Massive and diffusely graded polylithic breccias (Br/m/p) and Massive sandstones (St/m) (Table 4)

Massive and diffusely graded polylithic breccias (*Br/m/p*). Breccias develop voluminous outcrops characterized by the dominance of volcanic lithoclasts as well as fragmented crystals (Fig. 8d). They can reach 75 m thick (eg. in the Chaschuil section, Fig. 5) and beds are tabular, laterally extensive, with relatively sharp basal contact. Breccias are poorly sorted, matrix supported and dominated by lavic components. These breccias locally display gradual changes at the middle portion (up to 5 m), turning into a finer breccia enriched in andesitic-dacitic fragments, commonly imbricated.

Massive sandstones (*St/m*). Form tabular beds up to 1 m thick and nearly 20 m of lateral development (Fig. 5), overlying the *Br/m/p* with a sharp contact. Sandstones are massive, with volcanic clasts and feldspar fragments.

Interpretation: the features described for the *Massive diffusely graded polylithic breccias* (*Br/m/p*), such as the high concentrations of rock fragments of different shapes and sizes, the massive and diffuse changes in grain sizes and sharp contacts among others, point to define these deposits as debris flows. These deposits are awarded to very rapid movement or flow of non-plastic debris (boulder, rock and aggregate) in steep terrain (cf. Hürlimann et al. 2019). The gradual changes in grain size and/or clasts percentage in these breccias, may result from variations in the flow velocity mainly related to slope variations and/or incorporation of water (Fisher 1971; Nemec and Steel 1984). Changes in composition (dominance of andesitic-dacitic lithics) may reflect changes related to the source. The *Br/m/p* deposits studied along the Chaschuil area were defined as high concentration volcaniclastic debris flows (Cisterna and Coira 2014).

Inversely graded polymictic breccias (*Br/g/p*) and *Mudstones and fine sandstones* (*Mdt-St/s*) (eg. Chaschuil section, Fig. 5) (Table 4)

Inversely graded polymictic breccias (*Br/g/p*). Breccias, in sharp contact to the other units, are poorly sorted and the dominant clasts are dacites and rhyolites, scarce andesites, basalts and mudstones intraclasts (Fig. 8g). They have textural variations across the beds (with reverse and normal graded portions), being coarser and clast-supported at the central portion of the deposits. The presence of lava lithoclasts, plagioclase and quartz lithoclasts and abundant ash content is remarkable. To the top, breccias are interbedded with mudstones and fine crystal-rich sandstones (*Mdt-St/s*).

Mudstones and fine sandstones (*Mdt-St/s*). Crystal rich normally graded sandstones and mudstones beds to the top, forming tabular sets up to 70 cm thick and continuous laterally development up to 80 m.

Interpretation: the *Br/g/p* breccia deposits, comparable with the *Br/m/p* breccias, reflect an environment dominated by effective fragmentation, mainly composed by volcanic material, without evidences of a hot gas-supported

Table 4 Resediment syn-eruptive volcaniclastic facies: summary

Lithotype	Code	Description	Depositional processes
Massive and diffusely graded polymictic breccias	(*Br/m/p*)	Coarse massive, matrix supported (clast matrix volcaniclastic 35–40%), polymitic breccia at the base, grading to fine lithic breccias (clast matrix 5–10%) at the top. Characterized by the dominance angular to subangular of lava lithic clasts (dacites, andesites and minor basalts), less common are welded ignimbrites, lithic and crystallolithic tuffs. Large lithoclasts up to 30 cm long are at the basal portion. Crystal fragments in the matrix (up to 15%), usually broken, are plagioclase and quartz. Other components are glass shards. The finer top of the breccia is richer in fragments of andesitic-dacitic composition and clasts are locally aligned. Coarse to fine sand matrix with the same composition of the clasts and enriched in pyroclastic material	Debris flows
Massive sandstones	(*St/m*)	Massive coarse sandstones with subangular to subrounded lithic clasts commonly lavic (the same compositions related to the (*Br/m/p*) and feldspar fragments (5%). Pelitic and fine sandstone matrix, with high content of volcanic material (eg. glassy shards, pumice), recrystallized quartz, feldspar and quartz fragments, granophyric lithoclasts. Chlorite	
Inversely/normally graded polymictic breccias	(*Br/g/p*)	Polymictic poorly sorted breccias with sandy to muddy matrix with reverse and normal graded. Clasts, subangular–subrounded, are dominated by dacites and rhyolites. Breccias display textural variations across the beds, at the base have 20% of lithic clasts (between 1 and 15 cm large) in a fine sandy matrix. Proportions and size change into 40% and 2–40 cm long, at the central portion of the deposits. The matrix is a greyish-green sandy to greenish muddy, having fine lava lithoclasts, plagioclase and quartz fragments. The ash content is remarkable, with preserved cuspate relict glass shards, partly silicified. Locally the muddy matrix develops laminated and convolute structures	Debris flows and turbidity currents
Mudstones and fine sandstones	(*Mdt-St/s*)	Mudstones and fine crystal-rich sandstones. Sandstones are diffusely graded and have thick between 10 and 40 cm. Mainly composed by volcanic lithics, feldspar and quartz fragments and pyroclastic material	

Table 4 (continued)

Lithotype	Code	Description	Depositional processes
Diffusely graded polymictic breccias	(*Br/po/g*)	Lithic breccias form diffusely graded and form discontinuous beds. Clasts are subangular (up to 15 cm). Commonly are at the base and to the top poorly sorted (with 30% clasts), at the middle massive and matrix-supported (with 5–10% clasts). The breccia composition is the same that of the sandstones (*St/ml*)	Low and high density turbidity currents
Massive and laminated Sandstones	(*St/ml*)	Sandstones, fine to pebbly, may be massive to poorly stratified, or diffusely normally graded. Sandstones have plagioclase and quartz fragments, subangular volcanic clasts (andesitic, dacitic, rhyolitic, less common ignimbrites) and mudstones intraclasts of 1.5 cm. Commonly muddy matrix with glass shards partially altered to chlorite and/or siliceous aggregates with axiolitic textures. Fluid escape structures at the top of the beds	
Laminated siltstones	(*Sl/l*)	Green and thinly parallel laminated, siltstones commonly show mud intraclasts, erosive and scoured basal boundaries between them and the mudstone levels. Convolute bedding and fluid escape structures at the base and top of beds are common	
Massive and laminated siltstones	(*Mst/ml*)	Green to greyish-green, massive or laminated. Accretionary lapilli, with zonation (up to 5 mm) are frequently in the laminated mudstones levels. Massive mudstones commonly silicified	
Pyroclastic rich laminated siltstones	(*pySl/l*)	Tabular beds of fine laminated siltstones, up to 30 cm thick. Microscopically show chloritized portions of glass and pumiceous material silicified, glass shards	Syn-eruptive water-settled fallout deposits
Pyroclastic rich fine to pebbly sandstones	(*pySt/g*)	Fine to pebbly sandstones normal graded, with nearly 15% clasts (up to 4 cm size). Pyroclastic rich deposits (crystals fragments, glass shards and lapillies with preserve quenched margins) and minor lavic fragments, in a recrystallized vitroclastic matrix with abundante pumiceous material	

mode of emplacement. Characteristics as poor sorting, dominantly massive nature, reversely graded base and presence of a muddy matrix point to a deposition from cohesive debris flows (cf. Hampton 1972; Lowe 1982; Nemec and Steel 1984). To the top, the finer beds with laminated structures showing interstratified crystal-rich normally graded sandstones and mudstones, suggest transformations from debris flow deposits to turbidites. Flow transformation may be related to the incorporation of water into the system and/or with changes in high slopes where turbulence is produced and a decrease in flow density is recorded (Komar 1971).

Volcaniclastic mudstones, siltstones, fine to pebbly sandstones and fine breccia (Table 4)

Mudstones, siltstone and fine to coarse sandstones massive and laminated (*Mst/ml*)-(*Sl/l*)-(*St/ml*) are interbedded. Commonly, at the base are diffusely laminated mudstones and fine sandstones, with sets between 1 and 20 cm thickness reaching to 20 m total thick (Figs. 8f and 9). Gradually change to the top into poorly sorted fine to pebbly crystal-rich sandstones (up to 30 cm thick) interbedded with fine laminated mudstones and siltstones. Towards the top, diffusely graded coarse sandstones dominate. Lithic volcanic

Table 5 Volcanogenic sedimentary facies: summary

Lithotype	Code	Description	Depositional processes
Vitric fine-graied sandstone and siltstone	(*vSt/g*)-(*vSl/l*)	Fine sandstones and siltstones normally graded with wide compositional volcanic clasts (nearly 20%), displaying different nature (andesitic, dacitic, rhyodacitic, granophyric, granitic, mudstones). In thin sections are recognized crystal fragments of plagioclase and quartz, glassy shards and pumice floating and rarely, very fine schists, in a fine grained quartz-feldspathic groundmass	Low density turbidity currents
Laminated fine sandstones and siltstones	(*St/l*)-(*Sl/l*)	Laminated fine sandstones and mudstones, tabular beds up to 4 m thick, bedded on mm-dm scale, displaying ripple-cross bedding and climbing ripple sets. Locally syn-sedimentary deformational structures, commonly ball and pillow types. Fossils, mainly represented by a brachiopod fauna	Suspension deposition, storm and wave action
Thinly laminated mudstones and siltstones	(*Mst/l*)-(*Sl/l*)	Thinly laminated mudstones and siltstones. Relict glass shards were recognized microscopically	Suspension fall-out

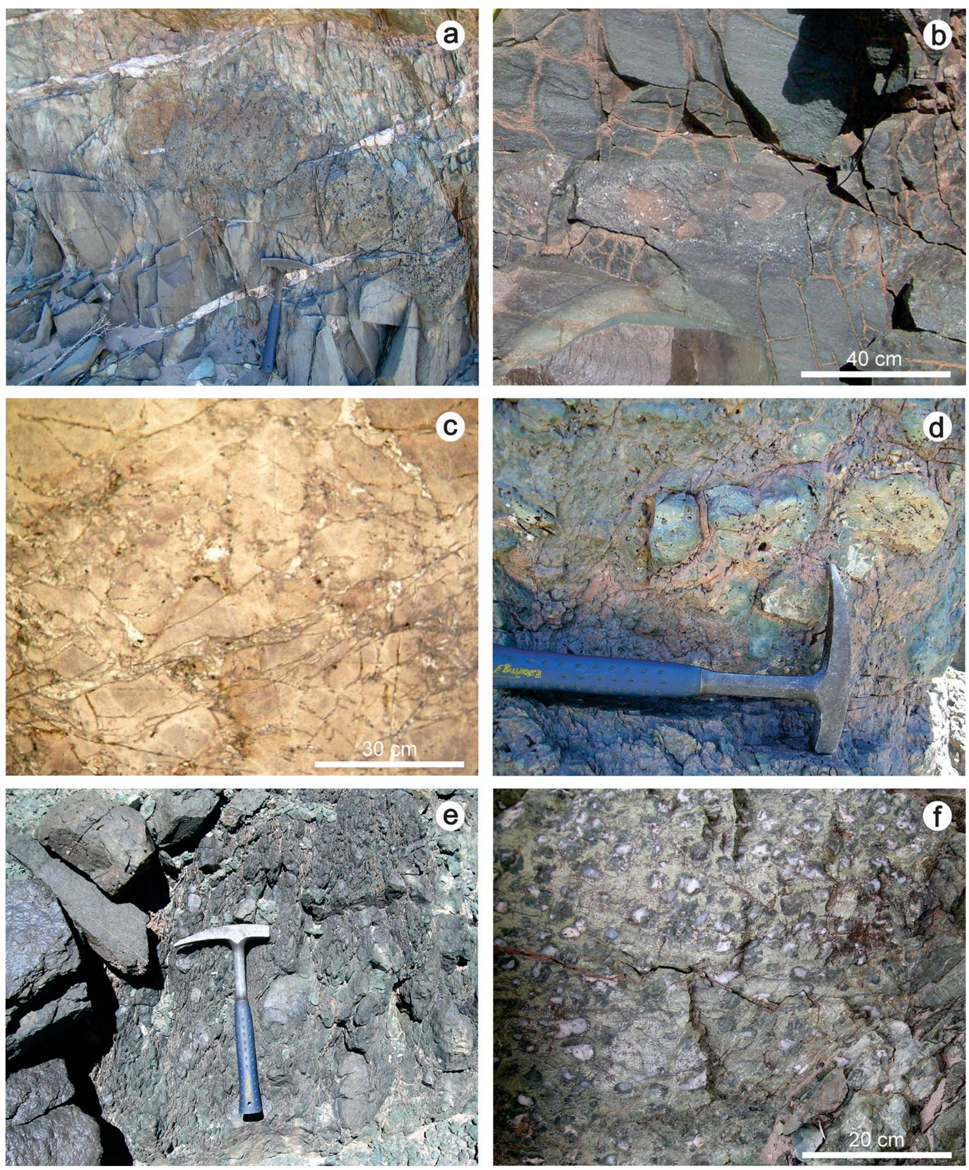

Fig. 6 **a** Contact between massive basalt and hyaloclastite with high vesiculated clasts of basalt. **b** Autoclastic basalt displaying jigsaw texture and a dyke of groundmass rich in in situ hyaloclastite. **c** Basalt showing jigsaw texture and growth of calcite among the clasts. **d** Basaltic hyaloclastite. Clasts of different size, blocky and with margins not quenched. Clasts and groundmass contain abundant vesicles. **e** Brecciated basalt displaying flow structure. **f** Dacitic breccia, fragments partially replaced by calcite and quartz

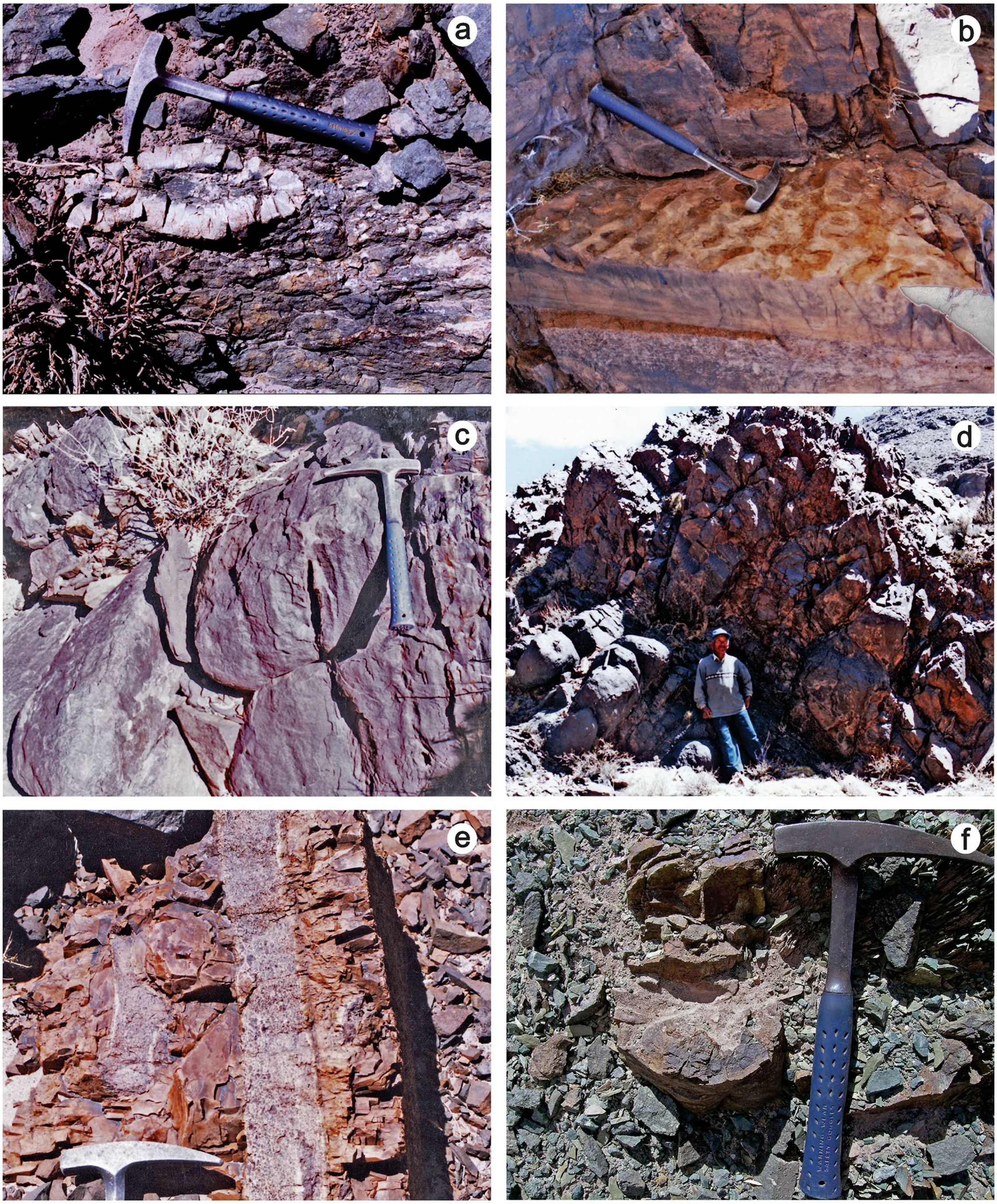

Fig. 7 **a** Fragmented basaltic outcrops in the Vuelta de Las Tolas (see Fig. 2). Clasts are rimmed by calcite. Agua del Médano section (see Fig. 2) showing: **b** Contact between basalt and a fine sandstone showing current-ripples structure. **c** Ropy wrinkles developed in the same basalt outcrop. **d** Basaltic outcrop pillowed and slightly deformed. **e** Fine sandstone intruded by basaltic lavas and reaction zones. **f** Pillow lobe segment with a glassy rind margin and flow wrinkles. Weak development of radial joints

clasts range between 10% at the basal levels and up to 25% to the top. The matrix has abundant pyroclastic material. Beds have fluid escape structures at the top.

Laminated and massive mudstones, *siltstones and fine to pebbly sandstones* (*Mst/ml*)-(*Sl/l*)-(*St/lm*). Thinly parallel laminated siltstone, fine sandstone and mudstones couples occur interstratified with parallel beds of fine sandstones (up to 30 cm thick)**.** Sandstones develop graded bedding that change to the top into pebbly and poorly sorted sandstones, interbedded with laminated mudstones lenses. Lithic clasts are lavic (andesites, dacites, rhyolites, 25% in average) and lesser amounts of pyroclastic material (ignimbrites and glass shards). Broken crystals of quartz and plagioclase are other components.

Laminated and massive mudstones, *siltstones*, *fine sandstones and polylithic breccia* (*Mst/ml*)-(*Sl/l*)-(*St/ml*)-(*poBr/g*) (Fig. 11a). n sharp contact to the other units, basal beds are mudstones displaying fluid escape structures on top of beds, massive and parallel laminated (total thickness up to 25 m). Mudstones are rich in devitrified glass fragments (15% in average). Interbedded, siltstone layers (sets up to 30 cm thick) display convoluted structures, have mud-intraclasts and developed erosive to scoured basal boundaries. Sandstone beds are moderately to poorly sorted and show planar lamination. The main components are volcanic clasts (reaching 35%), fragmented crystals (5–15%), very fine pumice fragments and recrystallized shards. Polylithic breccias develop interbedded as lenses (up to 60 cm), they are diffusely graded and have the same composition as the sandstones.

Interpretation: the analyzed deposits show characteristics such as the centimeters scale layering, sharp basal contacts and very long extension of the outcrops together with its sheet-like geometry that point to define them as turbidities. They are dominantly formed with fine-grained sandstones to mudstones, commonly normal graded and have lenticular coarser beds that may represent channel-fill settings (cf. Allen 1985). In the Chaschuil section, these deposits were defined as eruption-fed turbidity currents (Cisterna and Coira 2014) and, according their textural variations were recognized low and high density turbidity currents (greater concentration of particles and coarser clasts in high density ones).

Pyroclast- rich siltstones and fine to pebbly sandstones (pySl/l))-(pySt/g)

They form tabular units up to 10 m thick (Fig. 8h), composed by fine laminated green siltstones (sets up to 30 cm) interlayering with fine to pebbly sandstones normally graded. They develop tabular beds between 30 and 50 cm thick. It is remarkable the abundance of pyroclastic materials (crystals fragments, glass shards and lapilli, Fig. 11b) and recrystallized vitroclastic matrix. In the Punta Pétrea area (Fig. 2) were recognized fine sandstone beds (up to 40 cm thick) with abundant accretionary lapilli reaching 2.5 cm long.

Interpretation: the high content of pyroclasts components and an internally graded and massive structure, together with the absence of bed lenticularity, scouring, clast imbrication and cross-stratification in these deposits indicate that they may be subaqueous suspension fall beds (cf. White 2000).

Volcaniclastic sedimentary sandstones and siltstones with interbedded breccias facies (Table 5)

Mainly composed by laminated mudstones, siltstones and sandstones, are characterized by the presence of reworked clasts of volcanic source together with others of different nature (e.g. mudstones, granites, fine schists). Other volcanogenic deposits locally recognized in the same area, are pebbly sandstones and pebbles forming discontinuous beds up to 10 m thick.

Vitric fine-grained sandstone and siltstone (*vSt/g*)-(*vSl/l*) develops tabular beds that are stacked forming packages up to 20 m thick, where fine sandstones and siltstones layers range from 15 to 30 cm thick. Beds have sharp bases and tops and to the upper portion, sandstone beds develop normal grading structures and are common fluid escape structures.

Laminated fine sandstones and siltstone (*St/l*)-(*Sl/l*). Locally developed, beds are tabular developing up to 4 m thick, characterized by the current mega-ripples structures with nearly 20 cm of amplitude (Fig. 11c).

Thinly laminated mudstone and siltstone (*Mst/l*)-(*Sl/l*) develops up to 25 m thick. Tabular beds commonly display a millimeter-thick parallel lamination in sets up to 30 cm thick.

Interpretation: vitric fine-grained sandstone and siltstone (*vSt/g*)-(*vSl/l*) were interpreted as sediments that would have been transported by low concentration silty-muddy turbidity currents (Mángano and Buatois 1997). Suspension fall-out coupled with traction transport was indicated by the *Thinly laminated mudstone and siltstone* (*Mst/l*)-(*Sl/l*) (Cisterna and Coira 2014). The pebbly sandstones and pebbles discontinuous beds were interpreted as channel deposits (Mángano and Buatois 1997).

Lithofacies associations

Lithotypes are genetic and spatially related forming the main lithofacies associations along the region, they are: (1) Basic to intermediate lavas and their fragmented equivalents facies; (2) Rhyodacitic and rhyolitic lava domes/sills and rhyolitic dykes; (3) Resediment syn-eruptive volcaniclastic facies; and (4) Volcanoclastic sedimentary sandstones and siltstones with interbedded breccias facies.

Basic to intermediate lavas and their fragmented equivalents facies

Integrated by the Basaltic lavas (*BaL*), Monomictic basaltic breccias (*BaBr/m*), Basaltic pillow breccias (*BaPilBr*),

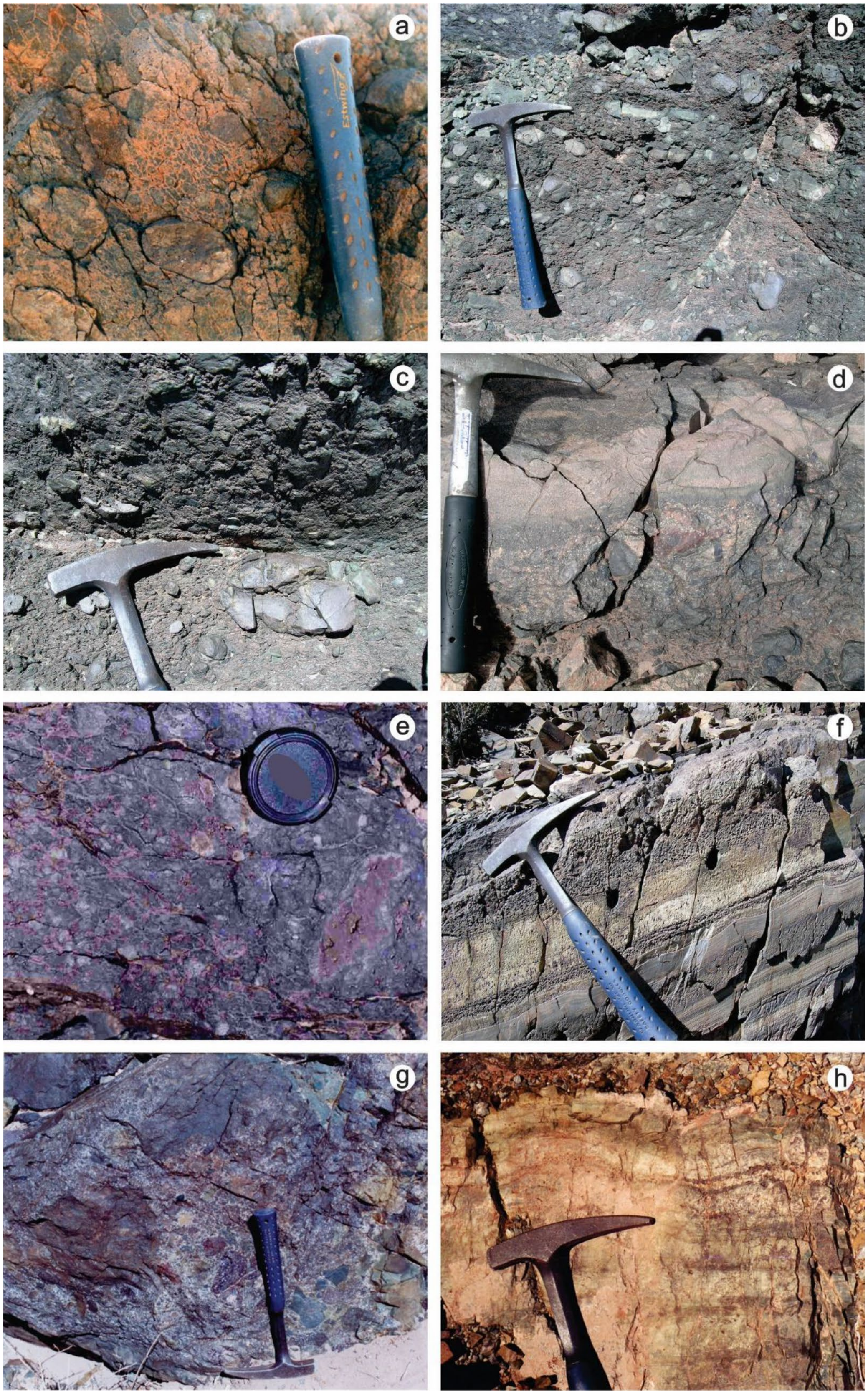
a
b
c
d
e
f
g
h

◂**Fig. 8** **a** Basaltic breccia mainly composed with pillows (*BaPilBr*), related to pillow lavas emplacements. **b** Sharp contact between basaltic breccia deposits (*BaBr*). They were deposited from debris flow near to the source. Locally clasts are imbricated. **c** Detail of the contact between basaltic breccias, showing flow structure and abundant vesicles. They were formed under high temperatures. **d** Contact between basaltic hyaloclastite (*BaBr*) and polylithic breccia (*Br/m/p*) interbedded with sandstones to the upper portion. **e** Massive polylithic breccias (*Br/m/p*) locally dominated by andesitic and dacitic lithoclasts. **f** Laminated mudstones, siltstone and fine sandstones massive and laminated (*Mst/ml*, *Sl/l*, *St/ml*) showing abundant fluid escape structures. **g** Polymictic breccias (*Br/po/g*) poorly sorted, with subangular volcanic clasts (dacitic, rhyolitic, andesitic, basaltic) and mudstones intraclasts. **h** Siltstones interbedded with fine sandstones (*pSl/l*, *pSt/g*) slightly folded

Andesites and dacites lava (*AnDaL*), Andesitic and dacitic breccias (*AnDaBr*), and *Basaltic breccias* (*BaBr*) lithotypes, this association represents the main volumes of basaltic lava flows, autoclastic breccias and hyaloclastites facies outcropping along a nearly north to south narrow area from Agua del Médano to the south of the Sierra de Las Planchadas (Fig. 2). They are characterized by their compositional affinity because up to 90% is basaltic, both lavas and breccias.

Interpretation: this lithofacies association, including massive and fractured lavas, pillow lavas and hyaloclastic deposits is the product of subaqueous emplacements, as was testified by their preserved textures and structures. South of the Quebrada Larga area (Fig. 2), basalts and basaltic breccias are intercalated with marine fossiliferous sediments, testifying the emplacement of the flows in an Ordovician submarine environment (Cisterna et al. 2017). The Basaltic breccias (*BaBr/m*) are in situ hyaloclastites, as was stated on the basis of their poorly sorted and chaotic deposits and considered proximal facies and formed next to its source. Taking into account clasts characteristics, angular and fusiform with glassy rinds commonly preserved, may be considered as syn-eruptive deposits possibly related to the development of spaces opened up in the lava flow, places where commonly temporary vents cause the hydro-magmatic activity (cf. Carr and Jones 2001). Related to hydromagmatic episodes because of water-magma interaction, relieving the pressure on the underlying melt, may be related to the mixture of fragments in the (*BaBr/m*) (either massive and angular or highly vesiculated and with glass rinds). They result from the relieving of pressure on the underlying melt, because of the sudden unmixing of the volatile component and to consequent magmatic fragmentation (cf. Dellino and La Volpe 1995). The unsorted and unstratified nature of the Basaltic pillow breccias (*BaPilBr*) and its proximity to the pillow-basalts point to weakly inclined slopes (cf. Allen et al. 2007). Basaltic breccia (*BaBr*) deposits, showing lack of vertical grading and discontinuous lensing distribution of the beds, suggest deposition of coarse clasts as bed-load lags and the scarce of finer components may imply that environment was too erosive to deposit or preserve sand component during its developing (cf. Allen et al. 2007). Sandstone bed-lenses preserved within breccias may be formed when flow lost turbulence. The discontinuous and lensoidal beds and its textural and structural characteristics indicate that they probably represent debris flow deposits infilling channels (Fig. 8b).

Rhyodacitic and rhyolitic lava domes/sills and rhyolitic dykes

The *Rhyodacitic and rhyolitic lava-domes/sills* are mainly emplaced along the southwestern and south of the Sierra de Las Planchadas area (Fig. 2) and the *Rhyolitic dykes*, intruding the entire Ordovician stratigraphic column, are included in this facies on the basis of their petrographic and chemical affinities (Cisterna and Coira 2017).

Interpretation: rhyodacitic and rhyolitic lavas were considered as shallow emplaced sills and small domes (Cisterna and Coira 2017). Domes, with scarce development of autoclastic texture or lack of related hyaloclastic facies suggest an emplacement in shallow water and/or subaerial. The presence of the oxidized portions proves that at least some of them were subaerial eruptions. *Rhyolitic dykes* may be temporally related with the *Rhyodacitic and rhyolitic lava domes/sills* due they are the only Ordovician units where they are not intruding.

Resediment syn-eruptive volcaniclastic facies

They are mainly represented by breccias, developing very thick deposits up to 75 m thick and composed by lavic or by lavic and pyroclastic clasts, interbedded with sandstones, siltstones and mudstones. Voluminous outcrops of these facies are along the eastern flank of the Sierra de Las Planchadas and between Chaschuil to Vuelta de Las Tolas localities (Fig. 2). Along the Chachuil area (eg. Chaschuil section), Cisterna and Coira (2014) interpreted these facies as water supported mass flows submarine deposits, such as turbidity currents and debris flows related to an environment where gravity and seismic episodes continuously act as instability factors. At the present study, facies defined by Cisterna and Coira (2014) at the Chaschuil section are redefined taking into account new data from there and from other localities. Lithofacies associations are:

Massive and diffusely graded polylithic breccias (*Br/m/p*) interbedded with *massive sandstones* (*St/m*). Outcrops are discontinuous and extend from the Quebrada Larga area to the southwest, at the west of Chaschuil (Fig. 2), along up to 8 km. The (*Br/m/p*) breccias are the dominant deposits.

Interpretation: the *massive polylithic breccias* result from relatively high concentration debris flow which clast size variations mainly denote energy fluctuations and high slopes

Fig. 9 Basaltic breccias (*BaBr/m*), interbedded with fine stratified sandstones (yellow) and siltstones (green-grey) (*Mst/ml*, *Sl/l*, *St/ml facies*). South of the Quebrada Grande area

reliefs morphologies. Flows deceleration give place to the interbedded massive sandstones. These deposits may have developed close to the volcanic edifices and fluctuations in energy could be explained with the seismic activity related to the volcanism. The (*Br/m/p*) interbedded with (*St/m*) have similarities with the coarse breccia-conglomerate dominates deposits and secondary interbedded pumiceous pyroclastic and sandstone units described by Allen et al. (2007) for the facies developed along proximal apron sections in volcanic areas. The juvenile nature of the breccia components, together with the structure and large thickness of the deposits (several meters), point to that they are the products of contemporaneous lavic and explosive eruptions, accompanied by sloughing of debris from the flanks of active volcanoes. Taking into account the juvenile pyroclastic components, these deposits were interpreted as formed close to intrabasin mesosilicic volcanoes that possibly generated explosive eruptions in shallow submarine or subaerial environments (Cisterna and Coira 2014).

Inversely/normally graded polymictic breccias (*Br/g/p*) interbedded with *mudstones and fine sandstones* (*Mdt-St/s*). These deposits were recognized from the Quebrada de La Gallina Muerta to the south, until 27°49´S. They are also outcropping in the north, in the Agua del Médano area (Fig. 2).

Interpretation: the (*Br/g/p*) breccias, showing gradations and turning into turbidity currents to the top, reflect flow dynamics variations, possible related to the incorporation of water or to changes in velocity flow due to slope variations (Fisher 1971; Nemec and Steel 1984). The finer upper beds, indicating a more dilute transport system, are typically related with debris flows developed along submarine aprons (Allen and Freundt 2006). The (*Br/g/p*) *and* (*Mdt-St/s*) facies may be compared with deposits related to medial position on submarine aprons described by Allen et al. (2007).

Volcaniclastic mudstones, *siltstones*, *fine to pebbly sandstones and fine breccia lenses* (*Mst/ml*)-(*Sl/l*)-(*St/ml*)-(*poBr/g*). Tabular beds (up to 45 m thick) are massive and laminated mudstones, siltstones and sandstones, locally interbedded with fine breccia lenses (e.g. Chaschuil section, Fig. 5). These facies were defined and detailed analyzed along the Chaschuil section (Cisterna and Coira 2014), where they have continuous outcrops and great extensional development (up to 3 km). To the north, in the Agua del Médano area, outcrops are abundant but discontinuous.

Interpretation: the *Volcaniclastic mudstones*, *siltstones*, *fine to pebbly sandstones and fine breccia lenses* represent low and high density turbidity currents deposits formed by the movement and sediment of sand and mud covering the continental shelf, mainly induced by the volcanic and/or seismic activity (cf. Yincan et al. 2017). Along the Chaschuil section, these facies were associated to directly and rapid deposition from dense suspensions and the coarser components were explained as probably transported in a highly concentrated traction carpet and in suspension at the base of the flow (Cisterna and Coira 2014). High-density turbidity currents are able to transport gravel and coarse sand material, mainly as a traction carpet at the base of the flow and in suspension just above. Fluid turbulence, dispersive pressure from grain collisions, and finer sediment exerting a matrix buoyancy life, keep the gravel and sand moving until the flow decelerates through increasing slope or dilution (Shanmugam 2019). Turbidity currents facies are comparable to the thick, pumiceous or pebbly sandstone interbedded with

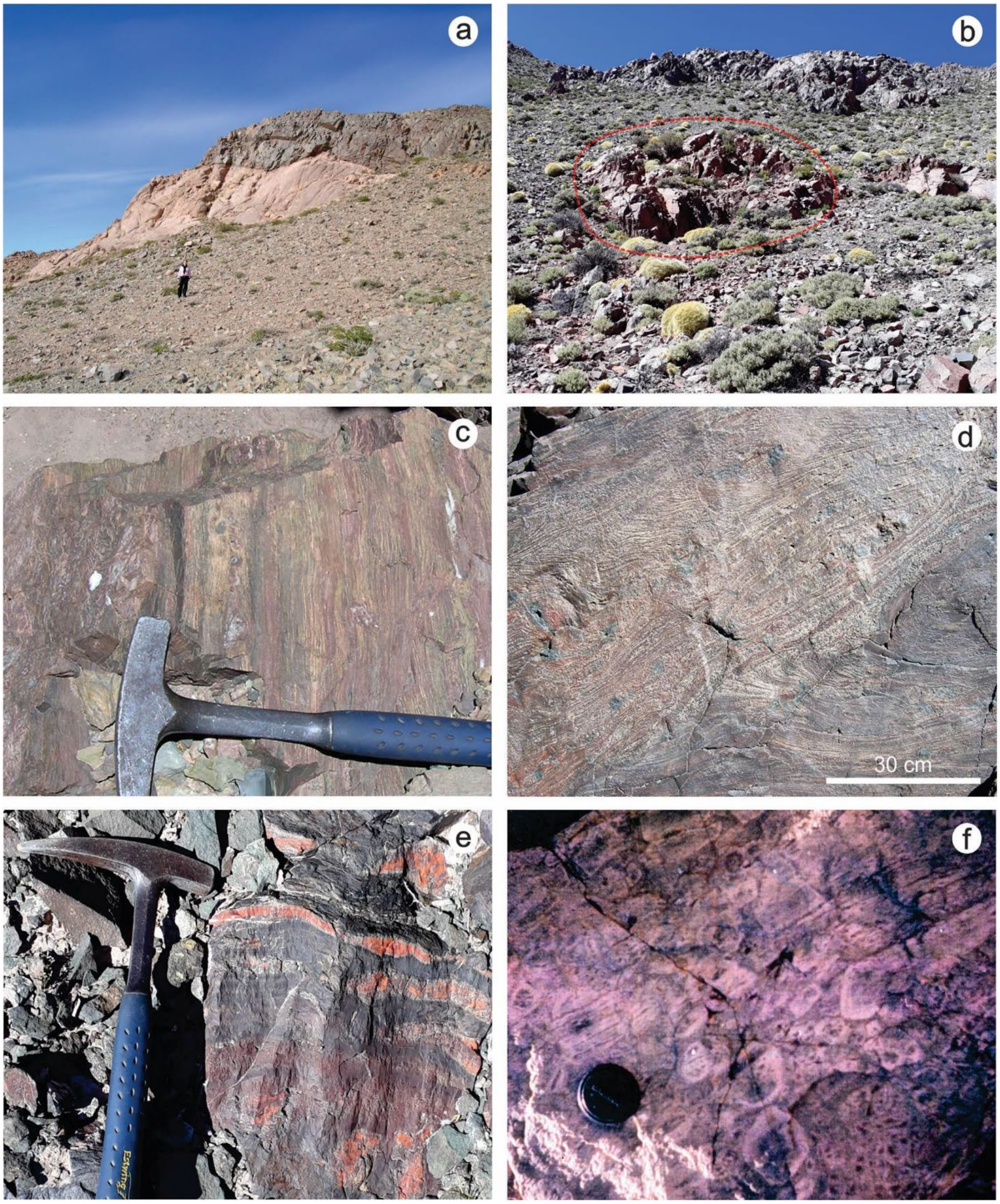

Fig. 10 **a** Rhyolitic red sills emplaced in volcaniclastic deposits in the Chaschuil are (see Fig. 2). **b** Rhyolitic dome emplaced in turbidity deposits of the *resediment syn-eruptive volcaniclastic facies*. Outcrop position is the northwestern side of the Chaschuil area (see Fig. 2). **c** Planar flow foliation in a rhyolitic lava-dome. **d** Rhyolitic lava with flow foliation structures that record its internal movement. Changes in the color and direction of the flows could be reflecting variations in the direction of the lava emplacement. Flow laminae are deformed around early-formed lithophysae. Small black fragments among lavas are similar to basaltic enclaves present in the rhyolitic dykes. **e** Rhyolite showing red oxidized zones as a result of subaerial conditions. **f** Flow banding in a devitrified rhyolite. White bands are devitrified centers replaced by quartz and green ones are altered feldspar and chlorite. Locally the lava is fragmented

intervals of fine-grained mudstone facies and rare beds of poorly sorted conglomerate described by Allen et al. (2007) in the distal part of a submarine volcaniclastic apron.

Pyroclastic rich siltstones and fine to pebbly sandstones (pySl/l))-(pySt/g) facies. Recognized at the east

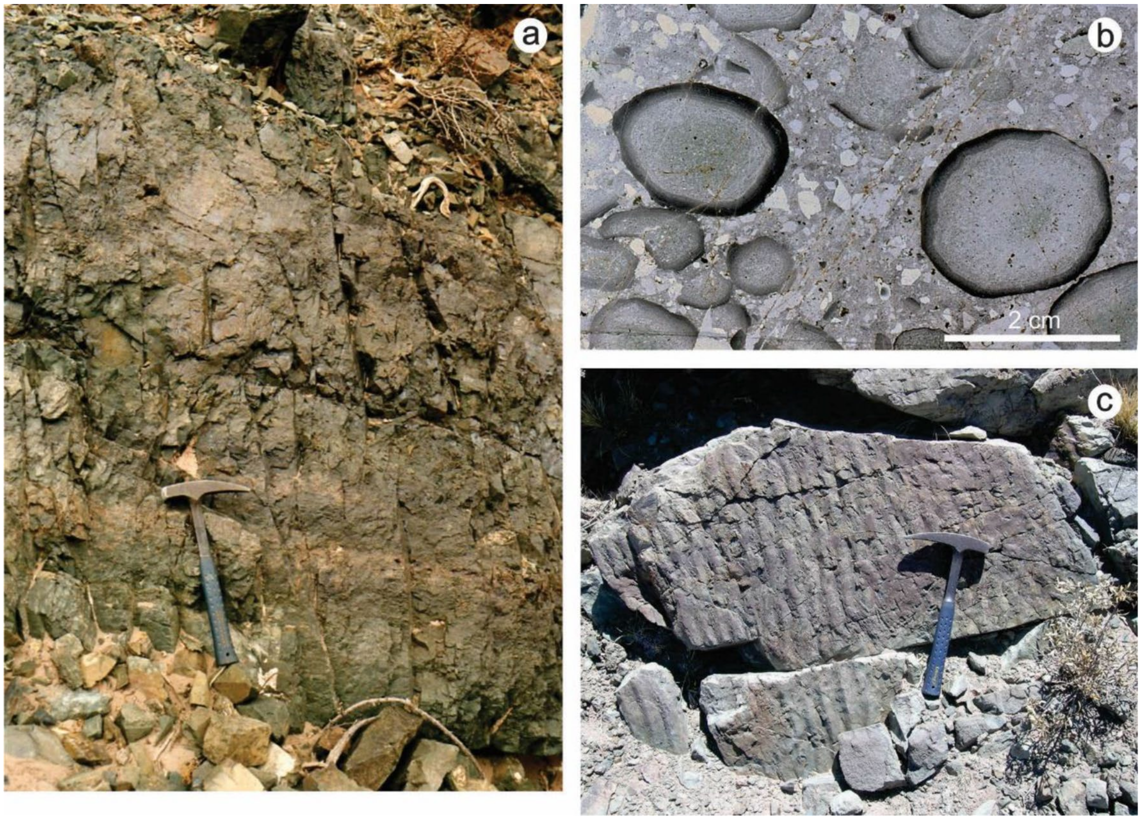

Fig. 11 **a** Mudstones, siltstones and fine sandstones succession deposited from turbidity currents (*Mst/ml*, *Sl/l*, *St/ml*, *poBr/g*). **b** Whole and lesser broken accretionary lapilli occurring in a fine sandstone, some of them preserving the outer finer rims (*pSt/g*). **c** Shallow water structures in fine facies of the volcanogenic sedimentary deposits (*St/l*, *Sl/l*)

of the Chaschuil, it covers nearly 200 m of discontinuous outcrops extending from NNE to SSW direction.

Interpretation: taking into account that these units, previously defined as subaqueous suspension fall beds, are composed entirely of pyroclastic products may be considered as resediment syn-eruptive volcaniclastic water settled deposit (cf. McPhie et al. 1993). Likewise, the important volume of shard components points to relatively rapid deposition, before the action of the ocean currents (cf. Stewart and McPhie 2004). The residence time of the suspended load may be turned greatly reduced by action of convective instabilities in one or more high-particle concentration layers in the water column, giving place to the settled of the finest pyroclasts through the water column may have been accelerated (cf. Carey 1997). The well preserved and abundant accretionary lapilli in some layers (eg. Punta Pétrea area) point to a source related to subaerial phreatomagmatic eruptions.

Volcanoclastic sedimentary facies

This facies outcrop at different places along the Sierra de Las Planchadas, however the most voluminous sections are located to the north, in Agua del Médano area (Figs. 2 and 7a) and at the southeastern and south sectors (e.g. along the Chaschuil section, a detailed study was made by Mángano and Buatois 1996, 1997).

Interpretation: the *fine-grained sandstone and siltstone* (*vSt/g*)-(*vSl/l*) *and thinly laminated mudstone and siltstone* (*Mst/l*)-(*Sl/l*) were include in the facies A and D of the Vuelta de Las Tolas member by Mángano and Buatois (1997) and interpreted as low concentration silty-muddy turbidity currents and that were formed by suspension fall-out coupled with traction transport, respectively (Cisterna and Coira 2014). The shallow-water depositional environment (above storm wave-base) is recorded in the *laminated fine sandstones and siltstone* (*St/l*)-(*Sl/l*) *deposits*. These facies were considered as the end of the sedimentation evolution of the basin and defined as the reworking volcaniclastic facies (Cisterna and Coira 2014).

Discussion

The Suri-Las Planchadas Volcanic-Sedimentary Complex (SPVSC) provides a complete record of the evolution from effusive mafic to intermediate submarine volcanism together with acid effusive and shallow intrusive facies, likewise the abundance of the pyroclastic material mainly composing the volcaniclastic facies point to pyroclastic activity. The Ordovician (Floian–Dapingian) age of the volcanism is indicated by the fossiliferous content (Albanessi and Vaccari 1994; Benedetto 1994; Vaccari and Waisfeld 1994) in the finer clastic members, interbedded among the volcanic rocks. Geochronology data obtained from a rhyolitic dome (Chaschuil area) indicated 468.3 ± 3.4 Ma for this facies (Baldo et al. 2003; Fanning et al. 2004). The association of volcanic members together with resedimented syn-eruptive volcaniclastic facies and volcanogenic sedimentary ones represents an excellent example to understand the architecture of this ancient volcanic complex and the characteristics of the volcanic and sedimentary processes involved in its evolution.

Tectonic environment: volcanism-sedimentation

The SPVSC was related to the evolution of an arc-back arc volcanic-tectonic system (Cisterna and Coira 2017; Cisterna et al. 2017). Basaltic lavas were related to subduction tholeiitic basalts showing similar characteristics that have been observed for example, in volcanic rocks of the Central American Volcanic Arc (Cisterna et al. 2017). They were also compared with basic effusions products of the transition from volcanic arc to extension related volcanism (back-arc) developed from progressive thickening of the overriding plate (cf. Morgan et al. 2008; Wehrmann et al. 2014). Basaltic, andesitic and dacitic lavas together with volcaniclastic debris-flow deposits and/or turbidities showing similarities to the SPVSC were studied in northeast Honshu, northeast Japan arc and explained as the result of the evolution of an arc-back arc system during Miocene–Pliocene (Yagi et al. 2009).

Rhyodacitic and rhyolitic lavas of the SPVSC were compared with volcanic arc effusions, related to subduction zones involving cortical elements (Cisterna and Coira 2017). Similar magmatic products were recorded in the Ediacaran Serie Negra Group of Ossa-Morena (590–545 Ma), which display oceanic environments with island-arc affinity linked to back-arc basins (Ribeiro et al. 2013; Sánchez Lorda et al. 2013; Padel et al. 2017).

Resedimented syn-eruptive volcaniclastic facies together with volcanogenic sedimentary facies of SPVSC complex were constructed along a submarine margin where episodic and strong seismic activity related to the volcanism gave rise to a high erosional environment where water supported mass flows deposits dominated (Cisterna and Coira 2014). Mass flow deposits are the proof of the recurrent periods characterized by high rate of sedimentation, strong slope control and instability episodes in the basin, typical of those volcanic environments (cf. Fisher 1966). The Ordovician mass flow deposits defined in the SPVSC complex show similarities with modern ones (e.g. Miocene Manukau Subgroup, New Zealand), related to a submarine volcaniclastic apron accumulated around a large, basaltic-andesitic volcanic island complex (Allen et al. 2007). Volcaniclastic debris-flow deposits and/or turbidities formed along a submarine apron were also described by volcanoes that grew from intermittent submarine eruptions of mafic to intermediate and/or felsic magmas (eg. the Fukuyama Volcanic Rocks) as in the back-arc Akita–Yamagata sedimentary basin in the Early to Middle Miocene arc-back arc opening of the Japan Sea (Yagi et al. 2009).

Facies characteristics as elements to define the complex's architecture

As was indicated for other modern and ancient volcanic active margins, facies analysis of volcanic type associations helps to reconstruct the architecture of the volcanoes and their evolution. Vertical and lateral downslope variations in the deposits commonly testified volcanic edifices erosion type and characteristics of the volcanism (cf. Allen et al. 2007). The Ordovician SPVSC, displaying a great variety of volcanic lithologies and volcaniclastic deposits with original textures, structures and field relations, represents an excellent example of volcanism related to the evolution of arc environment. The main volumes of the basaltic lava flows, autoclastic breccias and hyaloclastites facies along a nearly north to south narrow area (Fig. 2) possibly defines a continuous axis of submarine volcanic centers that currently cannot be recognized. Mafic effusions were subaqueous, as shown by the well-preserved structures indicatives of non-explosive magma-water interaction (Cisterna et al. 2017) and probably effusions began at deep levels, according the characteristics of the small outcrops of hosting mudstones only observed in North Quebrada Larga Section (Fig. 2). The close spatial association with basaltic lavas, hyaloclastites and rapid lateral facies variations (*basaltic breccias*) indicate an environment where submarine basalt flows are locally hydrobrecciated at their margins developing in situ hyaloclastite deposits (e.g. Fig. 4a). The resedimented hyaloclastic debris flows interfingering and locally mixing with the other basaltic facies are developed on a high-angle

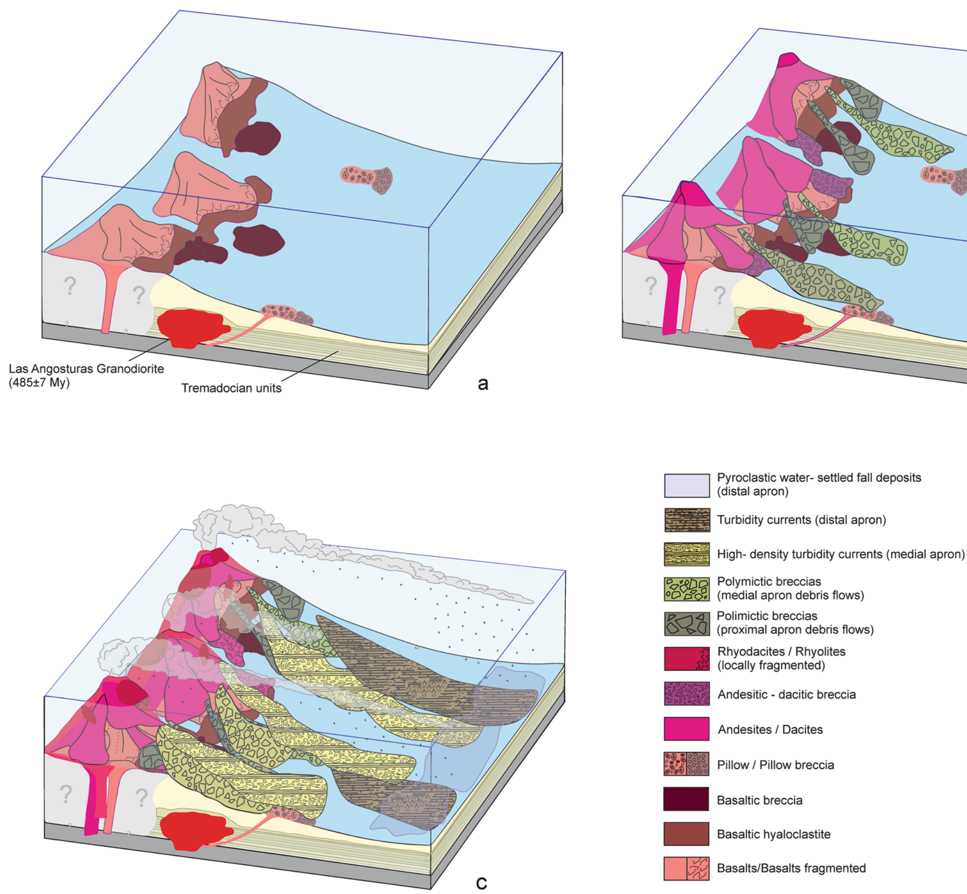

Fig. 12 Schematic reconstruction of the SPVSC evolution: **a** Submarine basaltic emplacements along an island arc. Lava–water interactions produced in situ hyaloclastic deposits. As the volcanic vents grew due the continuous volcanism, the surrounding apron developed high-angle slopes and resedimented hyaloclastic debris flows were formed in the proximal apron. **b** Continuity in the volcanism produce the grew and emergence of the volcanoes above the sea-floor, together with the magma evolution from mafic to intermediate. Instabilities along the arc and the beginning of subaerial erosion produce flow mass processes giving rise to debris flow deposits into the proximal and medial apron. **c** Felsic lavas and pyroclastic material contributed to the developing of the mass flow deposits formed along the medial and distal apron (resulting from debris flow and turbidity currents). Water-settled fall deposits were also formed in the distal apron

slope apron. *Basaltic breccia facies* (*BaBr/m*)—(*Babr*) testify high efficiency of fragmentation related to their source. The juvenile nature of the components and high bed thickness (several meters) point to eruptive and explosive volcanic activity with contemporaneous sloughing of debris from the flanks of the active volcanoes contemporaneous explosive and eruptions, together with sloughing of debris from the flanks of the active volcanoes (Fig. 12a). The lensoidal basaltic breccia bodies probably represent channels between lava lobes which have been infilled with hyaloclastic and other debris records. As the mafic and mafic to intermediate lavas repeatedly effused (as is registered along the South Quebrada Larga–Punta Pétrea section, Fig. 4a) were continuously forming hyaloclastic breccia deposits and the volcanic apron, surrounding the volcanic centers, was enlarged (Fig. 12b). The dacitic magma could have explosively erupted from the shallow-water dome or from emerging vent. Explosive activity was followed by eruption of relatively degassed magma to form the rhyodacitic–rhyolitic lava domes and sills (Fig. 12c). Likewise, recurrent calm periods could allow the accumulation of lenses of silt and sandstone interbedded among the volcanic records.

The SPVSC is characterized by a great development of mass flow deposits along the apron, which study allows to interpret their position related to the source, the slope of the apron, instabilities episodes during volcanism and volcanic processes. Submarine aprons are wedges of shallow-water to pelagic sediment deposits where clastic facies have little vertical organization. Lobes of talus, showing beds thinning and fining upwards, may be recognizable reflecting the development and evolution of submarine canyons and gullies as conduits for sediment transport from the upper to lower slope (Tucker et al. 1990). The sedimentary processes evolve gradually from slides on the slope, to a variety of sediment-gravity sheet flows over the aprons, and then to turbidity-current sheet flows reaching the basin-plain areas

(Weimer and Link 1991). In submarine aprons related to volcanic environments, high rates of sedimentation influence the architecture of the volcaniclastic apron and the facies characteristics reflects eruptive style, inter-eruption hiatuses and uplift events in the source volcanic island complex (cf. Allen et al. 2007). The dominant transport mechanisms are debris avalanches, debris flows and high-density and dilute turbidity currents. The debris flow deposits represented by the facies *Massive and diffusely graded polylithic breccias* (*Br/m/p*) interbedded with *Massive sandstones* (*St/m*) were compared to records developed along proximal apron sections. The debris flow and turbidity currents deposits of the facies *Inversely/normally graded polymictic breccias* (*Br/g/p*) interbedded with *Mudstones and fine sandstones* (*Mdt-St/s*) were compared as the records of the medial position on the submarine apron. Finally, *Volcaniclastic mudstones*, *siltstones*, *fine to pebbly sandstones and fine breccia lenses* (*Mst/ml*)-(*Sl/l*)-(*St/ml*)-(*poBr/g*) facies, representing gravelly high-density, sandy high-density and low-density turbidity currents deposits were compared as those described by Allen et al. (2007) in the medial and distal part of submarine volcaniclastic aprons.

Taking into account the composition of the different volcaniclastic facies defined in the SPVSC, almost all of them show dominance of lava components, pointing to a main effusive activity under subaqueous and subaerial conditions. Nevertheless, the continuous presence of pyroclastic material in these facies may suggest explosive eruptions associated to shallow water or to subaerial vents. The occurrence of accretionary lapilli in the matrix or as a main component in sandstones (up to 2.5 cm) and siltstones could be consistent with locally emergent phreatomagmatic volcanism, accompanied by a subaerial eruption plume.

Volcaniclastic deposits (resulting from debris flows and turbidity currents) composed by lava and pyroclastic fragments are the proof of contemporary explosive and effusive volcanic processes, with contribution of material resulting by the instability of the flanks and consequently landslides of the active volcanoes and / or of previous mass flow deposits along the apron. The facies associations defined in the SPVCS are comparable with others from volcanic arc settings along the world, largely controlled by the arc growth (cf. Fisher 1966; Fisher and Schmincke 1984; White 2000; Yagi et al. 2009).

Taking into account the proximity to source, the different resedimented syn-eruptive volcaniclastic facies display characteristics useful to indicate its position along the apron. Proximal apron facies were defined as debris flows represented by the *Massive and diffusely graded polylithic breccias* (*Br/m/p*) interbedded with *Massive sandstones* (*St/m*). They are characterized by the dominance of coarse and angular to subangular volcanic fragments, poorly selected and normal to inverse graded (cf. Walker 1984), where the nature of the clasts (dacites, andesites and minor basalts, less common pyroclastic ones) reveal subaerial or shallow water lava emplacements. Subaerial environments, especially shoreline ones, promote erosion and creation of steep cliffs that aid breakage of the lava into jointed clasts. Clast abrasion is more efficient in streams and above wave base than in deep water. Scattered throughout the coarse-grained facies are angular clasts mainly of basic lavas that have been derived from hyaloclastites and/or basaltic breccias. The pyroclastic components of the volcaniclastic facies, mainly in the matrix, point to a felsic subaerial or shallow subaqueous explosive concomitant volcanism. Similar mass flow deposits, dominated by clasts derived from subaerial lavas and texturally immature are related to submarine proximal apron originated from an actively growing volcano where lavas at the shoreline formed steep topographic gradients in volcanic island arc (cf. Allen et al. 2007) and volcanic arc-back arc systems (cf. Yagi et al. 2009).

The SPVSC also records mass flow deposits that according to their characteristics are related to medial and distal aprons. Medial facies are dominantly by polymictic breccias (*Inversely/normally graded polymictic breccias*, *Br/g/p*, and *mudstones and fine sandstones*, *Mdt-St/s*) deposited from debris flows and by mudstones, siltstones and sandstones with minor fine breccias (*Volcaniclastic mudstones*, *siltstones*, *fine to pebbly sandstones and fine breccia lenses*, *Mst/ml*, *Sl/l*, *St/ml*, *poBr/g*), deposited from high-density turbidity currents. Distal facies are dominated by thin-bedded sandstone and mudstone deposited from low-density turbidity currents in a relatively deep-water environment commonly interbedded with suspension fall-out rich pyroclastic facies. The mass flow facies assigned to a medial and distal apron deposition include abundant pyroclastic components, as lithic fragments and in the matrix, probably related to an increase of a concomitant explosive volcanism (Fig. 12c). Clasts of the acid lava members (rhyodacites and rhyolites) also common in these facies, testified the evolution to a felsic volcanism possible subaerial and/or in shallow water conditions.

Basaltic lavas emplacing in distal turbiditic sedimentary facies could indicate that basic volcanism was widespread from the arc axis and was continuous in time. In the *Vitric fine-grained sandstone and siltstone* (*vSt/g*, *vSl/l*) (distal facies) of the volcaniclastic sedimentary deposits, are outcrops of fragmented basalts emplaced in fine stratified beds (e.g. Vuelta de Las Tolas, see Fig. 2).

Water-settled fall deposits (*Pyroclastic-rich laminated siltstones and fine to pebbly sandstones*, *pySl/l*, *pySt/g*, siltstones and fine to pebbly sandstones facies) are interbedded with the turbidity current facies (e.g. Fig. 5). The significant volume of shard composing beds could indicate that deposition was relatively rapid, before ocean currents redistribute it (cf. Stewart and McPhie 2004) and possible concomitant with an explosive volcanism.

During the periods of quiescence between eruptions, occurred the abrasion and reworking of volcanic fragments and accumulation of normal sediments on the volcaniclastic apron. Fine-grained volcaniclastic sedimentary facies interbedded with coarse volcaniclastic mass flow deposits and minor with basaltic lavas, represent low-energy environment deposition. Facies defined as dilute turbidity currents deposited in distal areas are interbedded with very fine pyroclastic rich fall deposits (Mángano and Buatois 1997). Facies composed of siltstones and fine sandstones developing ripple-cross bedding and, rarely, climbing ripple sets suggest a shallow-water environment, above storm wave-base and possibly in a tidal setting. All of these facies are rich in pyroclastic components suggesting a continuous contribution, directly or indirectly, from explosive felsic volcanism. Channel incisions occurring along the apron and infilled by coarse volcaniclastic deposits were related to the apron uplift (Mángano and Buatois 1997). They may be principally constructed from deposits of high-energy sediment gravity flows (mainly turbidity currents and debris flows) as terrigenous and shallow marine sediment is redistributed into deeper water (cf. Deptuck and Sylvester 2018).

The SPVSC in the regional context

The Suri–Las Planchadas Volcanic-sedimentary Complex, in the northern portion of the Famatina System (Fig. 1b, c), represents the most complete and continuous records of the Famatinian volcanic arc-activity in the regional context. Although along the Famatina System were recognized discontinuous outcrops of volcanic and volcaniclastic Ordovician units that could be correlated with the SPVSC, today this is still a matter of discussion. At the central portion of the Sierra de Famatina (Fig. 1c) were defined Middle Ordovician units (Astini and Dávila 2002) consisting of rhyolites and rhyodacites emplacements locally brecciated and ignimbrites at the base (El Portillo Formation, Astini and Dávila 2002) and to the top, ignimbrites, tuffs with abundant lapilli and coarse to fine volcaniclastic deposits with abundant pyroclastic components, interbedded with marine epiclastic facies (sandstones, fine conglomerates, siltstones hosting brachiopods) all together defined as the La Escondida Formation (Astini and Dávila 2002). At the west of the Sierra de Famatina (e.g. Sierra de Toro Negro, Valle Hermoso, among others), Mannheim (1993) described volcanic rocks that could be correlated with the volcanic members of the SPVSC (Las Planchadas Formation). The dominant lithotypes are pyroclastic rocks (tuffs, ignimbrites), together with andesites, dacites, rhyolites and basalts. The succession has marine sedimentary deposits (shales, sandstones, siltstones, lime and reworking tuffs) included in the Suri Formation (Mannheim and Miller 1996). The shales host graptolites of Arenig age (Toselli et al. 1990). To the south, in the Chuschín area (Fig. 1c), were recognized volcanic-sedimentary deposits mainly composed by rhyolites and volcaniclastic breccias, together with tuffs, sandstones enriched in pyroclastic components and fine epiclastic facies. According to the fossil content, these deposits were assigned to the Arenig–Llanvirn (Mannheim 1993).

To the north of the analyzed area (Fig. 1b) were described small and isolated outcrops of the Ordovician units. At the Sierra de la Quebrada Honda were recognized basaltic to andesitic flows and dykes emplaced in fine marine sedimentary beds (Coira et al. 2009). The basalts and related hyaloclastic breccias are covered by Devonian sedimentary rocks (Coira et al. 2009). In the Sierra de Calalaste were described rhyolitic-dacitic emplacements and tuffs among sandstones and siltstones with graptolites, pointing to ages of Upper Arenig-Llanvirn (Zimmermann y Balhburg 2006).

The volcanic-arc records of the Famatinian belt are well represented in Puna (Fig. 1b), where two NNE-trending magmatic–sedimentary Ordovician belts (Eastern Eruptive Belt, EEB, and Western Eruptive Belt, WEB) are arranged. The older volcanic records in the WEB (Upper Cambrian-Lower Tremadocian) are represented by dacitic to rhyolitic lavas, hyaloclastites, tuffs, pyroclastic flows and minor amounts of basaltic lavas, related to the evolution of a marginal basin (Coira 2008). Meanwhile, in the EEB the volcanism represented by dacites and basalts to sub-alkaline microgabros, with E-MORB characteristics, signals the beginning of an active extensional regime with the development of a retro-arc basin with oceanic crust (Coira 2008). During the Floian-Darriwilian lapse, the volcanism in the WEB was characterized by the presence of basaltic to andesitic massive to pillow lavas and hyaloclastite breccias at the base, changing into dacitic to rhyolitic pyroclastic flows, lapillites and tuffs intercalated in the volcaniclastic turbidites sequences to the upper portion of the stratigraphic column (Coira and Koukharsky 2002). They show characteristics of arc to back-arc developed on a thin continental crust (Coira 2008). The bimodal magmatism recorded in the EEB during the Upper Tremadocian-Floian-Darriwilian reach its climax with siliceous syn-sedimentary lava-domes and sills with autoclastic breccias, hyaloclastites and minor spilitized basaltic pillow lavas, lacoliths and sills of microgabros. The intraplate signature of basic rocks and crustal filiation of siliceous rocks indicate a tectonic environment where the alkaline magmatism is the result of decompression of the mantle in an extensional environment, while an important crustal fusion takes place (Coira 2008).

The above points out that although there are Ordovician volcanic and volcaniclastic records that can be correlated with the SPVSC, further field, geochemical and geochronological studies are still needed, both in reference to the geological context of the Famatina System and also related to the Puna.

Conclusions

The SPVSC records the products of an Ordovician arc volcanism, starting with the emplacement of basaltic submarine effusions together with the development of related fragmented facies. Such mafic rocks were related to subduction systems and chemical data indicated tholeiitic effusions comparable to those of island arcs (Cisterna et al. 2017). As the volcanism evolves, initially basaltic effusions change into calc-alkaline andesites and dacites with arc-affinities and the final stages of the magmatic evolution is represented by the felsic subvolcanic and explosive volcanism. Rhyodacites and rhyolites chemical data indicate a source related to volcanic arcs-back-arc systems (Cisterna and Coira 2017). Along modern arcs (eg. the volcanic evolution of the Japan arc), submarine volcanoes grew through intermittent submarine eruptions of calc-alkaline, mafic to intermediate and felsic magmas generating associated volcaniclastic sediments of rock fragments derived from them. Together with the magma evolution during the growth of the volcanoes, from mafic to intermediate and felsic members, the eruptive pattern shifted from effusive to explosive eruption, producing a large apron of syn-and post-eruptive volcaniclastic deposits of debris flows and/or turbidity currents. These deposits are the testimony of variations in composition and volcanic style and contribute to the evolution of a volcanic apron from deeper to shallow water environments. Interfingering between the facies along the submarine apron allows to indicate progradation of the apron with the evolution of the volcanism. Volcaniclastic sedimentary shallow-water beds host fossils that testify the Dapingian–Floian age. The abundance of pyroclastic components in most of the volcaniclastic facies indicates that, at least the compositionally most evolved records derived from felsic subaerial or shallow subaqueous explosive volcanism.

Acknowledgements This study was supported by the Consejo Nacional de Investigaciones Científicas y Técnicas de Argentina (CONICET)—PIP N° 5115, Universidad Nacional de Tucumán (CIUNT) 26/G410, Agencia Nacional de Promoción Científica y Tecnológica (ANPCYT) PICT 7-8724 and Universidad Nacional de Jujuy (SECTER UNJu) 08/E015 Project. Our gratitude to Christoph Breitkreuz and an anonymous reviewer for their very intense work and valuable comments.

References

Aceñolaza FG, Toselli AJ (1976) Consideraciones estratigráficas y tectónicas sobre el Paleozoico inferior del Noroeste Argentino. II Congreso Latinoamericano De Geología, Caracas, Actas 2:755–764

Aceñolaza FG, Toselli A (1984) Lower ordovician volcanismin North West Argentina. In: Bruton DI (ed) Aspects of the ordovician system, vol 295. Palaeontological Contributions University of Oslo, Oslo, pp 203–209

Albanessi G, Vaccari E (1994) Conodontos del Arenigiano en la Formación Suri. Sistema de Famatina, Argentina. Rev Esp Micropaleontol 26(2):125–146

Allen JRL (1985) Principles of physical sedimentology. Springer, London, p 272

Allen SR, Freundt A (2006) Resedimentation of cold pumiceous ignimbrite into water: facies transformations simulated in flume experiments. Sedimentology 53:717–734

Allen RS, Hayward BW, Mathews E (2007) A facies model for a submarine volcaniclastic apron: the Miocene Manukau subgroup, New Zealand. Geol Soc Am Bull 119(5/6):725–742

Almeida F, Hasui Y, Brito Neves BB (1976) The upper Precambrian of South America. Univ Sao Paulo Inst Geosci Boletim 7:45–80

Altenberger U, Cisterna C, Günter C, Gutiérrez A, Rosales J (2021) Tectono-metamorphic evolution of the proto-Andean margin of Gondwana: evidence of internal high-grade metamorphism along the northern portion of the Famatinian orogen, Sierra de Aconquija, Sierras Pampeanas Orientales, Argentina. J S Am Earth Sci. https://doi.org/10.1016/j.jsames.2021.103305

Astini RA, Benedetto JL (1993) A collisional model for the stratigraphic evolution of the Argentine Precordillera during the early Paleozoic. In: 2° International Symposium on Andean Geodynamics (Oxford), Paris, p 501–504

Astini R, Dávila F (2002) El Grupo Cerro Morado (Ordovícico Medio) en el Famatina (28°-29° S), Andes Centrales del oeste argentino. Revista Geológica De Chile 29:241–254

Astini RA, Dávila FM (2004) Ordovician back arc foreland and Ocloyic thrust belt development on the western Gondwana margin as a response to Precordillera terrane accretion. Tectonics. https://doi.org/10.1029/2003TC001620

Astini RA, Benedetto JL, Vaccari E (1995) The early Paleozoic evolution of the Argentine Precordillera as a Laurentian rifted, drifted and collided terrane: a geodynamic model. Geol Soc Am Bull 107:253–273

Bahlburg H (1990) The Ordovician basin in the northern Puna of Argentina and Chile: geodynamic evolution from back-arc to foreland basin. Geotekton Forsch 75:1–107

Bahlburg H (1991) The Ordovician back-arc to forelands successor basin in the Argentinian-Chilean Puna: tectono-sedimentary trends and sea-level changes. Sedim Tectonics Eustasy Sea-Level Changes Active Mar 12:465–484

Bahlburg H (1998) The geochemistry and provenance of ordovician turbidites in the Argentinian Puna. In: Pankhurst RJ, Rapela CW (eds) The Proto-Andean margin of Gondwana, vol 142. Geological Society, London, pp 127–142

Bahlburg H, Vervoort JD, DuFrane A, Carlotto V, Reimann C, Cárdenas J (2011) The U-Pb and Hf isotope evidence of detrital zircons of the Ordovician Ollantaytambo formation, Southern Peru, and the Ordovician provenance and paleogeography of Southern Peru and Northern Bolivia. J S Am Earth Sci 32:196–209

Bahlburg H, Berndt J, Gerdes A (2016) The ages and tectonic setting of the Faja Eruptiva de la Puna Oriental, Ordovician, NW Argentina. Lithos 256–257:41–54

Baldo EG, Fanning CM, Rapela CW et al (2003) U-Pb Shrimp dating of rhyolite volcanism in the Famatinan belt and K-bentonites in the Precordillera. Ordovician from the Andes. Serie Correlación Geológica 17:41–46

Benedetto JL (1994) Braquiópodos ordovícicos (Arenigiano) de la Formación Suri en la región del Río Chaschuil, Sistema del Famatina, Argentina. Ameghiniana 31:221–238

Bierlein FP, Stein HJ, Coira B, Reynolds P (2006) Timing of gold and crustal evolution of the Palaeozoic south central Andes, NW Argentina-implications for the endowment of orogenic belts. Earth Planet Sci Lett 245:702–721

Carey SN (1997) Influence of convective sedimentation on the formation of widespread tephra fall layers in the deep sea. Geology 25(9):389–842

Carr PF, Jones BG (2001) The influence of palaeoenvironment and lava flux on the emplacement of submarine, near-shore Late Permian basalt lavas, Sydney Basin (Australia). J Volcanol Geoth Res 112:247–266

Chernicoff CJ, Zappettini EO, Santos JOS et al (2010) The southern segment of the Famatinian magmatic arc, La Pampa Province, Argentina. Gondwana Reseach 17:662–675

Chew DM, Schaltegger U, Košler J et al (2007) U-Pb geochronologic evidence for the evolution of the Gondwanan margin of the north-central Andes. Geol Soc Am Bull 119:697–711

Cisterna C, Coira B (2014) Subaqueous eruption-fed mass-flow deposits: records of the Ordovician arc volcanism in the Northern Famatina Belt; Northwestern Argentina. J S Am Earth Sci 49:73–84

Cisterna C, Coira B (2017) Registros volcánicos del magmatismo ordovícico en las provincias de Catamarca y La Rioja, noroeste de Argentina. Herramientas para la reconstrucción del arco famatiniano. In: Muruaga C, Grosse P (eds) Ciencias de la Tierra y Recursos Naturales del NOA. Relatorio Congreso Geológico, Tucumán, pp 414–433

Cisterna C, Mon R (2014) Episodios diastróficos ordovícicos registrados en las sucesiones volcánicas–sedimentarias del Tremadociano Temprano en el norte del Sistema de Famatina. Revista De La Asociación Geológica Argentina 71:393–403

Cisterna C, Coira B, Décima F (2010) Efusiones subácueas del arco volcánico ordovícico en el norte del Sistema de Famatina. Revista De La Asociación Geológica Argentina 66:223–235

Cisterna C, Koukharsky M, Coira B et al (2017) Arenigian tholeiitic basalts in the Famatina Ordovician basin, northwestern Argentina: emplacement conditions and their tectonic significance. Andean Geology 44(2):123–146

Clemens K (1993) Sedimentología, proveniencia y desarrollo geotectónico del Sistema de Famatina en el noroeste de Argentina durante el Paleozoico inferior. Congreso Geológico Argentino 2:310–321

Coira B (1979) Descripción Geológica de la Hoja 3C Abra Pampa, provincia de Jujuy. Servicio Geológico Nacional Boletín 170:1–90

Coira B (2008) Volcanismo del Paleozoico inferior en la Puna Jujeña. In: Coira B, Zappettini C (eds) Ciclo Pampeano—Famatiniano—Geología. Relatorio Congreso Geológico Argentino, Jujuy, pp 140–154

Coira B, Koukharsky M (2002) Ordovician volcanic activity in the Puna, Argentina. Aspects of the Ordovician system in Argentina. Serie De Correlación Geológica 16:267–280

Coira B, Pérez B (2002) Peperitic textures of Ordovician dacitic synsedimentary intrusions in Argentina's Puna Highland: clues to emplacement conditions. J Volcanol Geoth Res 114:165–180

Coira B, Davidson J, Mpodozis C, Ramos V (1982) Tectonic and magmatic evolution of the Andes of northern Argentina and Chile. Earth-Sci Rev 18:303–332

Coira B, Pérez B, Flores P, Kay S, Woll B, Hanning M (1999) Magmatic sources and tectonic setting of Gondwana margin Ordovician magmas, northern Puna Argentina and Chile. Spec Paper Geol Soc Am 336:145–170

Coira B, Koukharsky M, Ribeiro Guevara S, Cisterna C (2009) Puna (Argentina) and Northern Chile Ordovician basic magmatism: a contribution to the tectonic setting. J S Am Earth Sci 27:24–35

Currie C A, Hyndman R D (2005) The thermal structure of subduction zones: The case for a hot backarc: EOS. Transactions of the American Geophysical Union 86, abstract T11B-0366

Dalziel IWD (1997) Neoproterozoic Paleozoic geography and tectonics: review, hypothesis, environmental speculation. Geol Soc Am Bull 109:16–42

Dellino P, La Volpe I (1995) Fragmentation versus transportation mechanisms in the pyroclastic sequence of Monte Pilato-Rocche Rosse (Lipari, Italy). J Volcanol Geoth Res 64:211–231

Deptuck M, Sylvester Z (2018) Submarine fans and their channels, levees, and lobes. In: Micallef A et al (eds) Submarine geomorphology. Springer, Berlin, pp 273–299

Ducea MN, Otamendi J, Bergantz G et al (2010) Timing constraints on building an intermediate plutonic arc crustal section: U-Pb zircon geochronology of the Sierra Valle Fértil–La Huerta, Famatinian arc. Argentina Tectonics. https://doi.org/10.1029/2009TC002615

Fanning CM, Pankhurst RJ, Rapela CW et al (2004) K-bentonites in the Argentine Precordillera contemporaneous with volcanism in the Famatinian arc. J Geol Soc 161:747–756

Fisher RV (1961) Proposed classification of volcaniclastic sediments and rocks. Geological Society American Bulletin 72:1409–1414

Fisher RV (1966) Mechanism of deposition from pyroclastic flows. Am J Sci 264:350–366

Fisher RV (1971) Features of coarse-grained, high concentration fluids and their deposits. J Sedim Petrol 41(4):916–927

Fisher RV, Schmincke HU (1984) Pyroclastic rocks. Springer, Berlin, p 318

García-Ramírez CA, Rey-León V, Valencia V (2017) Ortoneises en la Franja Silos-Babega, Macizo de Santander, Colombia: evidencias de la orogenia famatiniana en los Andes del norte. Andean Geology 44:307–327

Hampton MA (1972) The role of subaqueous debris flow in generating turbidity currents. J Sediment Petrol 42(4):775–793

Hürlimann M, Coviello V, Bel C et al (2019) Debris-flow monitoring and warning: review and examples. Earth Sci Rev 199:1081

Komar PD (1971) Hydraulic jumps in turbidity currents. GSA Bull 82(6):1477–1488

Kraemer PE, Escayola MP, Martino RD (1995) Hipótesis sobre la evolución neoproterozoica de las Sierras Pampeanas de Córdoba (30°40′–32°40′ S) Argentina. Revista De La Asociación Geológica Argentina 50(1–4):47–59

Larrovere MA, de los Hoyos CR, Willner AP, et al (2019) Mid-crustal deformation in a continental margin orogen: structural evolution and timing of the Famatinian Orogeny, NW Argentina. J Geol Soc 177:233–257

Loewy SL, Connelly JN, Dalziel IWD (2004) An orphaned basement block: the Arequipa-Antofalla basement of the central Andean margin of South America. Geol Soc Am Bull 117:171–187

Lork A, Bahlburg E (1993) Precise U-Pb ages of monazites from the Faja Eruptiva de la Puna Oriental, NW Argentina. In: 12º Congreso Geológico Argentino and 2º Congreso Exploración de Hidrocarburos, Actas 4, p 1–6, Buenos Aires

Lowe DR (1982) Sediment gravity flows: II depositional models with special reference to the deposits of high density turbidity currents. J Sediment Petrol 52:279–297

Mángano MG, Buatois LA (1996) Shallow marine event sedimentation in a volcanic arc-related setting: the Ordovician Suri Formation, Famatina Range, northwest Argentina. Sed Geol 105:63–90

Mángano MG, Buatois LA (1997) Slope-apron deposition in an Ordovician arc-related setting: The Vuelta de Las Tolas member (Suri Formation), Famatina Basin, northwestern Argentina. Sed Geol 109:155–180

Mannheim R (1993) Génesis de las volcanitas eopaleozoicas del Sistema del Famatina, Noroeste de Argentina. In: 12 Congreso Geológico Argentino y 2 Congreso de Exploración de Hidrocarburos Actas 4, Mendoza, p 147–155

Mannheim R, Miller H (1996) Las rocas volcánicas y subvolcánicas eopaleozoicas del Sistema de Famatina. In Aceñolaza F et al.

(Eds.), Geología del Sistema del Famatina, Münchner Geologische 19 (A), pp. 159–186.
McPhie J (1995) A Pliocene shoaling basaltic seamount—Ba volcanic group at Rakiraki, Fiji. J Volcanol Geoth Res 64(3–4):193–210
McPhie J, Doyle M, Allen R (1993) Volcanic Textures: a guide to the interpretation of textures in volcanic rocks. In: CODES Key Centre, University of Tasmania, Hobart, Tasmania, p 198
Morgan JP, Ranero CR, Vannucchi P (2008) Intra-arc extension in Central America: links between plate motions, tectonics, volcanism, and geochemistry. Earth Planet Sci Lett 272:365–371
Nemec W, Steel RJ (1984) Alluvial and coastal conglomerates: Their significant features and some comments on gravelly mass-flow deposits. In: Koster EH, Steel RJ (eds) Sedimentology of gravels and conglomerates. Canadian Society of Petroleum Geologists Memoir, Calgary, pp 1–31
Niemeyer H, Gotze J, Sanhueza M, Portilla C (2017) The Ordovician magmatic arc in the northern Chile-Argentina Andes between 21° and 26° south latitude. J S Am Earth Sci 81:204–214
Padel M, Álvaro JJ, Casas JM et al (2017) Cadomian volcano sedimentary complexes across the Ediacaran-Cambrian transition of the Eastern Pyrenees, southwestern Europe. Int J Earth Sci. https://doi.org/10.1007/s00531-017-1559-5
Pankhurst R, Rapela C, Saavedra J et al (1998) The Famatinian magmatic arc in the Central Sierras Pampeanas: an early to midOrdovician continental arc on the Gondwana margin. The Proto-Andean Margin of Gondwana. Geol Soc London 142:343–367
Pankhurst R, Rapela C, Fanning H (2000) Age and origin of coeval TTG, I-and S-Type granites in the Famatinian belt of NW Argentina. Trans Royal Soc Edinburgh Earth Sci 91:151–168
Pankhurst RJ, Rapela CW, Fanning CM, Márquez M (2006) Gondwanide continental collision and the origin of Patagonia. Earth Sci Rev 76:235–257
Petersen CS, Leanza AF (1953) Elementos de geología aplicada. Nigar, Buenos Aires, p 475
Ramos V (1988) Late proterozoic-early paleozoic of South America: a collisional history. Episodes 11:168–175
Ramos VA (2018) The Famatinian orogen along the protomargin of Western Gondwana: evidence for a nearly continuous Ordovician magmatic arc between Venezuela and Argentina. In: Folguera A, Contreras Reyes E, Heredia N, Encinas AB et al (eds) The evolution of the Chilean-Argentinean Andes. Springer, Berlin, pp 154–183
Rapela CW, Pankhurst RJ, Casquet C et al (1998) The Pampean orogeny of the southern proto-Andes: evidence for Cambrian continental collision in the Sierras de CórdobaThe Proto-Andean Margin of Gondwana. Geol Soc London 142:181–217
Rapela CW, Pankhurst RJ, Casquet C et al (2018) A review of the Famatinian Ordovician magmatism in southern South America: evidence of lithosphere reworking and continental subduction in the early proto-Andean margin of Gondwana. Earth Sci Rev. https://doi.org/10.1016/j.earscirev.2018.10.006
Ribeiro JM, Stern RJ, Kelley K et al (2013) Nature and distribution of slab-derived fluids and mantle sources beneath the Southeast Mariana forearc rift. Geochem Geophys Geosyst. https://doi.org/10.1002/ggge.20244
Rubiolo D, Cisterna C, Villeneuve M (2002) Edad U/Pb del granito de Las Angosturas en la sierra de Narváez (Sistema de Famatina, provincia de Catamarca). In: 15 Congreso Geológico Argentino, Actas 1, Calafate, p 359–362
Sánchez Lorda ME, Sarrionandia F, Abalos B et al (2013) Geochemistry and paleotectonic setting of Ediacaran metabasites from the Ossa-Morena Zone (SW Iberia). Int J Earth Sci. https://doi.org/10.1007/s00531-013-0937-x
Shanmugam G (2019) Slides, slumps, debris flows, turbidity currents, hyperpycnal flows, and bottom currents. In: Kirk Cochran J (ed) Encyclopedia of ocean sciences, 3rd edn. Elsevier, New York, pp 228–257
Stewart AL, McPhie J (2004) An upper pliocene coarse pumice breccia generated by a shallow submarine explosive eruption, Milos, Greece. Bull Volcanol 66(1):15–28
Toselli A, Saavedra J, Pellitero E et al (1990) Geoquímica y petrogénesis del volcanismo ordovícico de la Formación Las Planchadas, Sistema del Famatina. Revista De La Asociación Geológica Argentina 45:13–32
Toselli A, Durand F, Rossi de Toselli J, Saavedra J (1996) Esquema de evolución geotectónica y magmática eopaleozoica del Sistema de Famatina y sectores de Sierras Pampeanas. In: 13 Congreso Geológico Argentino, Actas 5, Buenos Aires, p 443–462
Tucker M, Durham V, Wright P (1990) Carbonate sedimentology. Blackwell, Oxford, p 554
Vaccari E, Wasisfeld B (1994) Nuevos trilobites de la formación suri (Ordovícico Temprano) en la región de Chaschuil, provincia de Catamarca. Implicancias Bioestratigráficas Ameghiniana 31:73–86
Van der Lelij R, Spikings R, Ulianov A et al (2016) Palaeozoic to Early Jurassic history of the northwestern corner of Gondwana, and implications for the evolution of the Iapetus, Rheic and Pacific Oceans. Gondwana Res 31:271–294
Viramonte J, Becchio R, Viramonte JG et al (2007) Ordovician igneous and metamorphic units in southeastern Puna: new U-Pb and Sm–Nd data and implications for the evolution of northwestern Argentina. J S Am Earth Sci 24:167–183
Walker RG (1984) Turbidites and associated coarse clastic deposits. Facies Models. Geoscience 1:171–188
Wehrmann H, Hoernle K, Garbe-Schönberg D et al (2014) Insights from trace element geochemistry as to the roles of subduction zone geometry and subduction input on the chemistry of arc magmas. Int J Earth Sci 103:1929–1944
Weimer P, Link M (1991) Seismic facies and sedimentary processes of submarine fans and turbidite systems. Springer, New York, p 447
White JDL (2000) Subaqueous eruption-fed density currents and their deposits. Precambr Res 101:87–109
Yagi M, Ohguch T, Akiba F et al (2009) The Fukuyama volcanic rocks: Submarine composite volcano in the Late Miocene to Early Pliocene Akita-Yamagata back-arc basin, northeast Honshu, Japan. Sed Geol 220:243–255
Yincan Y (2017) Submarine turbidity current. Marine geo-hazards in China. Elsevier, Oxford, p 772
Zimmermann U, Balhburg H (2006) The Lower Ordovician Diablo formation (nom. nov.) in the southern Puna (NW Argentina): link between the northern Puna and the Sierra Famatina. Serie Correlación Geológica 21:171–196